Original Article

Histological Study of the Potential Therapeutic Effect of Bone Marrow Derived Mesenchymal Stem Cells Versus their Secreted Extracellular Vesicles on Rats' Seminiferous Tubules Following Busulfan Induced Toxicity

Reham A. Abdelrahman, Nadia A. Sharaf Eldin, Moushira Zoheir and Amany A. Solaiman

Department of Histology and Cell Biology, Faculty of Medicine, Alexandria University, Egypt

ABSTRACT

Introduction: Busulfan, an alkylating chemotherapeutic agent commonly used to induce myeloablation in leukemic patients, unfortunately leads to azoospermia and infertility in cancer sur*vivo*rs. Bone marrow derived mesenchymal stem cells (BM-MSCs) and their secreted extracellular vesicles (EVs) are emerging promising treatment modalities for treating testicular injury by busulfan.

Aim of the Work: To compare the therapeutic potential of BM-MSCs and EVs in attenuating histological and biochemical changes induced by busulfan on rats' seminiferous tubules.

Materials and Methods: Six young male albino rats were utilized for isolation of BM-MSCs and EVs. Fifty-eight adult male rats were divided into group I (control group) including 24 rats subdivided equally into 3 subgroups IA, IB&IC, group II (n=10, single I.P of 40mg/kg busulfan) 2 were sacrificed after 48 hrs for homing, group III (n=8, single injection of BM-MSCs 1x 10^6 cells/ 1 ml into the efferent ducts, group IV (n=8, single injection 40 µg MSC-EVs into the efferent ducts (&group V (n=8, left for recovery assessment), rats were sacrificed after 28 days. Blood and tissue samples were collected for biochemical analysis. Semen samples were obtained to measure sperm count and motile sperm percent. The testes were processed for light and electron microscopic examination and estimation of Johnsen score. Statistical analyses of the obtained data were performed.

Results: Busulfan induced disrupted architecture of seminiferous tubules with loss of spermatogenic cells with intercellular vacuolation and nearly empty lumina which was confirmed by ultrastructural findings. There was a statistically significant decrease in serum testosterone levels, antioxidant markers, sperm parameters and Johnsen score. Concurrently, there was a statistically significant increase in oxidant profiles. Treatment with BM-MSCs ameliorated histological & biochemical changes in seminiferous tubules. However, administration of EVs yielded better results.

Conclusion: EVs exhibited better therapeutic effects than BM-MSCs in alleviating busulfan induced testicular injury.

Received: 10 June 2024, **Accepted:** 09 August 2024

Key Words: Busulfan, BM-MSCs, extracellular vesicles, seminiferous tubules.

Corresponding Author: Reham Abdallah Abdelrahman, PhD, Department of Histology and Cell Biology, Faculty of Medicine, Alexandria University, Egypt, **E-mail:** rehamabdallah505@gmail.com

ISSN: 1110-0559, Vol. 48, No. 3

INTRODUCTION

Infertility is a major global health concern, about 12–15% of couples worldwide struggle with its consequences. Unfortunately, male infertility accounting for 50% of cases[1]. The number of cancer sur*vivo*rs has increased as a result of advancements in cancer detection and therapy. On the other hand, infertility is among the long-term side effects of chemotherapy. Alkylating drugs like cyclophosphamide, busulfan and cisplatin are frequently used in chemotherapy, and they have been linked to reduced sperm quality in cancer sur*vivo*rs. This can include decreased motility and count of sperms as well as an increase in abnormal morphology. These effects can last for years after cancer therapy is completed[2,3].

Busulfan (BU), also known as 1,4-butanediol methane sulfonate, is an anti-cancer medication used to treat lymphoma and leukemia. It is also frequently used in conjunction with other chemotherapeutic drugs for myeloablative conditioning prior to transplantation in patients receiving allogeneic hematopoietic cell transplantation (HCT)[4]. Through the alkylation of guanine nucleotides, BU hinders cell propagation and causes DNA to form cross links and solitary-strand interruptions[5].

The unique therapeutic potential of mesenchymal stem cells generated from bone marrow (BM-MSCs), including multilineage differentiation, immunomodulation as well as angiogenesis and anti-fibrotic effects, have made them a promising option in regenerative medicine[6]. However, there have been logistical obstacles in the way of converting these cells into clinical uses, including issues with large-scale production, viability and cell transport. Consequently, therapies based on extracellular vesicles (EVs) are gaining popularity as a new class of biological treatments that do not require cells[7].

DOI: 10.21608/ejh.2024.289766.2064

Extracellular vesicles (EVs) are membrane-bound cellular products that are secreted into the extracellular environment and have the ability to deliver signals to distant and neighboring cells[8]. Natural EVs are present in body fluids such as tears, blood, urine, saliva and breast milk. But mesenchymal stem cells can also be used to produce EVs on a massive scale[9].

Indeed, the contents of extracellular vesicles (EVs) vary based on how they arise and which particular cell they originate from. Major Histocompatibility Complex (MHC), integrins, membrane proteins, tetraspanins (CD9, CD63 and CD82), various categories of RNAs and lipids (ceramide, phosphatidylserine, sphingomyelin, and cholesterol) are all found in EVs[10].

Because of their nano size, high biocompatibility, minimal immunogenicity, effective cargo loading and ability to precisely target specific cells, extracellular vesicles (EVs) hold great therapeutic promise. Through their effects on angiogenesis, differentiation and proliferation of cells, they are essential in fostering tissue repair and regeneration[11,12]. Moreover, therapeutic medications can be encapsulated in EVs and delivered to certain target cells. The use of EVs as biomarkers to aid in illness detection has gained popularity recently[12,13].

MATERIAL AND METHODS

Chemicals

98% pure powdered busulfan (1,4-butanediol dimethane sulphonate) was purchased from SNF Medical Company in Egypt. Dimethyl sulfoxide (DMSO) and phosphate buffer saline (PBS) were mixed with the medication powder to form a solution.

Isolation of mesenchymal stem cells generated from bone marrow (BM-MSCs)[14, 15].

Six albino rats, two weeks old and weighing between 27 and 40 grams, were obtained for the study from the animal house of Alexandria university's physiology department. An excessive dose of anesthesia (100 mg/kg of phenobarbital) was used to euthanize rats. With a vertical laminar air-flow hood, the researchers used aseptic approach to extract bilateral femurs and the surrounding muscle tissues. Then, for two minutes, the femurs were submerged in 70% ethanol to disinfect them. After scraping off the muscles, PBS (Sigma, USA) was used to rinse the bones.

To extract bone marrow cell suspension, the femur's two ends were cut, and complete culture medium (CCM) was flushed into the marrow cavity. The cells from bone marrow were grown using complete media at 37 °C in a CO2 incubator with a dampened environment holding 5% CO2. Next, the mixture of bone marrow cells was filtered after that, the mixture was spun for a duration of five minutes[16]. Mesenchymal stem cells were employed in the third passage (P3) for this study. The cultured cells were observed through an inverted phase-contrast microscope.

Evaluation of BM-MSCs

Colony-forming unit-fibroblast (CFU-F) tests: to evaluate the ability of the cultivated cells to form colonies. 100 cells were placed in complete medium on a six-well plate for this test and left for a duration of 14 days. Every observable colony was examined using an inverted phase-contrast microscope. For MSC culture, a CFU potential greater than 40% was thought to be ideal[17].

Immunophenotyping Characterization using Flow Cytometer: Immunophenotyping was performed on cells at P3 after trypsinization. The cells were incubated with fluorescently labelled monoclonal antibodies (mAb) that were specific to the markers CD90 and CD45. Immunofluorescence on cells was examined using a FACS Calibur flow cytometer[18].

Isolation and purification of extracellular vesicles (EVs)[19]

Medium free of fetal bovine serum was used to cultivate the cells and incubated for a whole day afterwards, the conditioned media of BM-MSCs at P3 was collected. Following a 24-hour period, the medium was gathered, preserved at -80 °C, and later substituted with CCM. The following day, the CCM was substituted again with medium free of fetal bovine serum for another 24 hours, and this procedure was repeated every other day for 14 days.

EVs and the conditioned medium were separated by a differential centrifugation process. Initially, dead cells and cell debris were precipitated by centrifuging the sample and the resulting product was ultra-spun for a period of 70 minutes at 100,000 x g using a Beckman Coulter Optima XE-100 Ultracentrifuge (rotor 50.2 Ti) at the Institute of Graduate Studies and Research (IGSR), Alexandria University, to create an EVs pellet at 4 °C. Ultimately, in the laminar flow hood at CERRMA, the pellet was dissolved in 100 µl of sterile PBS to produce an EVs suspension.

Evaluation of EVs[20,21]

Zeta sizer nanoparticle analyser: At Alexandria University's Faculty of Pharmacy, the mean size of BM-MSCs-EVs was measured. In 1 milliliter of filtered PBS, 10 microliters of BM-MSCs-EVs were diluted for the analysis. Software for nanoparticle tracking analysis (NTA) was used to analyze the data from digital micrographs that had been acquired.

Transmission Electron Microscopy (TEM): The morphology and size of EVs were assessed by TEM (JEOL- JSM 1400 Plus, Japan). EVs were diluted with PBS in this procedure, and copper grids were coated with a drop of the solution. After being stained with 1% uranyl acetate and left to dry naturally afterwards, the specimen was examined.

At Alexandria University's Faculty of Medicine's Biochemistry Department, the Lowry technique was

applied to determine the whole amount of protein in the mixture of EVs.

Experimental design

Fifty-eight mature male albino rats, with weight range 200 to 250 gms, were kept in the Animal House. The Research Ethics Committee of Faculty of Medicine permitted the research ethics code for this study (serial number 0201750).

Rats were haphazardly divided as follows (Figure 1):

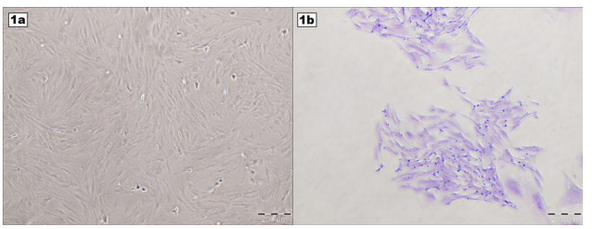

Fig. 1 (a,b): Phase contrast inverted microscopic photomicrographs of cultured BM-MSCs x100: a) Passage 3 showing 80-90% confluent spindle shaped fibroblast like cells. b) CFU assay of p3 cells with crystal violet stain showing 2 colonies.

Group I: Twenty-four rats were included in control group and sacrificed after 28 days of injection:

- Subgroup IA: 8 rats, each took a single intraperitoneal injection of 2 ml of dimethyl sulfoxide ("DMSO", vehicle of busulfan) diluted in phosphate buffer saline (PBS)[22].
- Subgroup IB: 8 rats were injected once with one ml of culture medium free of cells, vehicle of BM-MSCs into the efferent ducts of each testis[22].
- •Subgroup IC: 8 rats were injected once with one ml of phosphate buffer saline (vehicle of EVs) into the efferent ducts of their testes[23].

Group II: Eight rats, each rat was intraperitoneally injected by 40 mg/Kg body weight busulfan once. Later rats were put to death after 28 days[22].

Group III: Ten rats following 28 days from BU administration, on the 29th day, received a single injection of BM-MSCs within the culture medium (1x 10^6 cells/ 1 ml), into the efferent ducts of each testis.

Two randomly selected rats of this group were euthanized after 48 hours, for detection of homing of the cells in the seminiferous tubules. Fluorescent probe (chloromethyl - benzamide octadecyl indocarbocyanines, or CM-DiI) was applied to label BM-MSCs. Blue Hoechst 33342 stain Solution (20 mM) (Thermo Fisher, USA) was utilized to counterstain DNA. Confocal laser microscopy was used to visualize the labelled cells. The remaining 8 rats were euthanized after another 28 days[24,25].

Group IV: (Busulfan +extracellular vesicles derived from BM-MSCs group): Eight rats following 28 days from BU administration, on the 29th day, received a single dose of 40 µg MSC-EVs (dissolved in PBS) into the efferent ducts of each testis. The rats were euthanized after another 28 days[23].

Group V: (Recovery group): Eight rats following 28 days from BU administration, were left with no further intervention for another 28 days, and then they were euthanized, in order to assess the potentials for spontaneous recovery.

Sampling

All of the rats were put to death at the end of the study by intraperitoneal injection with 100 mg/kg of phenobarbital. To assess the levels of total antioxidant capacity (TAC) and testosterone, blood samples were gathered from the abdominal aorta and centrifuged to produce serum. The epididymides were removed and processed for sperm count and motile sperm percent. The right and left testes were excised and managed for histological examination. Also, testicular homogenate was prepared to determine malondialdehyde (MDA) and glutathione peroxidase levels.

Biochemical assessment

a) Hormonal assay of serum testosterone

Enzyme-linked immunosorbent assay (ELISA) kit (Chongqing Biospes, USA) was used following the kit protocol for the quantitative measurement of testosterone expressed in nmol/L[26].

b) The oxidant markers

Malondialdehyde (MDA) in tissue homogenate

As a marker of oxidative stress, MDA is a byproduct of lipid peroxidation. Testicular samples were homogenized ten times (w/v) in cold PBS with inhibitor of protease. The Humalyzer junior photometer (Human Diagnostics, Germany) was used for colorimetric analysis of MDA in nmol/gm tissue using kits from Bio diagnostic, Egypt[27].

c) The antioxidant markers

Serum total antioxidant capacity (TAC)

The antioxidative capacity was assessed by ELISA according to the manufacturer's protocol of Chongqing Biospes company. Results were expressed in U/ml[28].

Glutathione peroxidase in tissue homogenate

The colorimetric method was utilized via kits acquired from Biodiagnostic, Egypt in order to assess the glutathione peroxidase levels in testicular homogenate. The results were expressed in U/g tissue and the method was carried out in accordance with the manufacturer's instructions[29].

Epididymal sperm count & total sperm motility

Using sharp scissors, the dissected cauda epididymis from each rat was cut and placed in a preheated Petri dish with 1 ml of PBS. A sperm suspension was made by pipetting repeatedly. The suspension was then diluted with

PBS 1:20 for sperm counting on a hemocytometer slide. The total sperm count was calculated by counting the motile sperm and sperm in eight squares and multiplying the result by 5x104. To assess the total percentage of motility of the sperm, a single drop (50µl) of the suspension was put on a slide that had been pre-heated and inspected utilizing x400 lens of light microscope[30].

Histological examination

Light microscopic examination

All rats' right testes were first fixed for 24 hours in Bouin's solution, then they were fixed in 10% formol saline. After formation of paraffin blocks containing testicular tissues were sectioned at 5 µm thickness that were stained with hematoxylin and eosin (H&E) stain ,observed and photographed[31].

Johnsen score

The Johnsen score was used to evaluate the rats' seminiferous tubules. Based on a score ranging from one to ten for the maturity of the germ cells. Maximum spermatogenesis activity was reflected by a score of 10, while total absence of germ cells was indicated by a score of 1. The total number of scores was mathematically divided by the number of tubules analyzed to obtain the mean score[32].

Transmission electron microscopic examination

A portion of the left testis was cut into 1 mm3 cubes and preserved in 2.5% glutaraldehyde for ultra-structural analysis. After being rinsed, the specimens were post-fixed with 1% osmium tetroxide, dehydrated, and then embedded in epoxy resin and cut to form ultrathin (90 nm) sections for application of lead citrate and uranyl acetate dyes[33].

Statistical analysis

The data, including serum testosterone levels, oxidant and antioxidant markers, semen parameters, and Johnsen score, were analyzed using a statistical software application and shown as the mean plus or minus the standard deviation. ANOVA and post hoc tests were applied for statistical analysis. A statistically significant *p-value* was interpreted to be < 0.05.

RESULTS

Evaluation of BM-MSCs

At passage 3 showed confluent spindle fibroblast like cells reached 80-90% confluency (Figure 1a). CFU-F assay of BM-MSCs revealed small stained colonies on day 14 of passage 3. (Figure 1b). The results of the flow cytometric examination of the BM-MSCs' cell-surface markers showed that 98.94% of cells were positive for anti-CD44 and 98.92% of cells were positive for anti-CD90. No cells were detected positive for anti CD45 (Figures 2a,b).

Evaluation of extracellular vesicles

EVs appeared double layered membrane-bound spherical vesicles with different sizes by transmission electron microscopy (Figure 3a). The hydrodynamic size distribution of BM-MSCs-EVs was estimated by zeta sizer nanoparticle analyzer and average size was 225 nm peak diameter (Figure 3b). The average total protein content of the extracellular vesicles' (EVs) suspension was estimated to be 0.9 mg/ml using the Lowry method.

BM-MSCs homing within testicular tissue

Labelled BM-MSCs were traced in testes 48 hours after insertion into efferent ducts and observed by confocal laser microscope.BM-MSCs expressed red fluorescence of CM-Dil in their cytoplasm and tissue was counterstained in blue with DNA binding Hoechst stain (Figure 4).

Biochemical results

Serum testosterone

There was no statistical difference between subgroups IA, IB &IC of group I. The mean of serum testosterone was significantly lower in group II. Meanwhile in group III testosterone level boosted when compared to group II with no statistical significance between both groups. Nevertheless, after injection of group IV, a noteworthy elevation was noticed when compared to group II and III. Group V was significantly lower than group II (Figure 5a)

Oxidative stress marker malondialdehyde (MDA)

Tissue MDA levels showed significant increase in group II compared to subgroups IA, IB &IC. Moreover, mean values of groups III, IV &V were significantly higher than group I. MDA in groups III and IV were expressively less than group II. However, group IV was significantly lower. Additionally, there was a significant decline in MDA level in group IV in comparison to group III. The MDA of group V was expressively elevated than all other groups (Figure 5b).

Total serum antioxidant capacity (TAC)

The mean of serum TAC was significantly lower in group II when compared to subgroups IA, IB & IC. There was a noteworthy alteration between group I, III &V. Yet, in group IV the mean value was lower than subgroups of group I. In group III, there was significant increase in TAC level when compared to group II. Moreover, in group IV, a noteworthy rise in TAC level was detected in comparison to group II. Also, the mean value of group V was significantly lower than all groups (Figure 5c).

Glutathione peroxidase (antioxidant marker)

Tissue glutathione peroxidase levels exhibited significant decrease in group II and group V when compared to subgroups IA, IB& IC. furthermore, showing statistical difference between group II and V. However, the mean value of group III was slightly lower than group II with no statistical significance, but in group IV, the mean value had significantly dropped in comparison to control subgroups and it was significantly higher than groups II &III as well (Figure 5d).

Epididymal sperm count

Epididymal sperm count was almost the same in subgroups IA, IB, and IC. In contrast to the first group, groups II, III, and IV showed a considerable decline. The sperm count in group IV, exhibited a significant elevation compared to group III. However, this apparent increase in the sperm count was statistically still less than the mean value of subgroups IA, IB & IC. Moreover, group V showed significant decrease in mean value when compared to all other groups (Figure 6a).

Total percentage of sperm motility

The % of sperm motility did not vary by a significant margin amongst subgroups IA, IB, and IC.

Conversely, a statistically significant rise in the motile sperm percentage was observed in group IV in comparison to group III. Group V depicted a statistically significant lower total sperm motility percentage than all groups (Figure 6b).

Johnson score

A statistically significant lower Johnsen score was detected in group V and group II in comparison to rest of groups. Though, there wasn't statistical variance between subgroups IA, IB and IC. Furthermore, there was a noteworthy statistical variation among groups III and IV but still significantly lower than subgroups IA, IB and IC yet higher than group II (Figure 6c).

LM examination

Group I (Control group): Inspection of the seminiferous tubules by LM of group I, revealed normal histological findings, which were almost the same in the three subgroups (IA, IB, and IC). The germinal epithelium of seminiferous tubules comprising Sertoli cells and spermatogenic cells resting on regular basement membrane. Basal spermatogonia showed dark rounded nuclei. Huge, spherical nuclei with distinctive chromatin condensation were visible in primary spermatocytes. Multiple layers of early spermatids were detected with their pale rounded nuclei. Elongated spermatids & multiple spermatozoa were also seen. Sertoli cells showed pale nuclei and evident nucleoli. (Figure 7).

Group II (Busulfan group): Group II revealed by LM distorted seminiferous tubules with irregular thickened basement membrane. Widened lumen was seen with a decrease in the dark& widely separated spermatogenic cells lining the tubules. Some sloughed pyknotic cells were seen within lumen Sertoli cells showed cytoplasmic vacuolations. Leydig cells appeared scattered. (Figures 8a,b).

Group III (BM-MSCs group): Few areas of seminiferous tubules were improved showing organized arrangement of its cells with minimal intercellular spaces in between. Primary spermatocytes appeared with vacuolated cytoplasm. Few rows of early spermatids were depicted. Few vacuolations were present in between Leydig cells (Figure 9).

Group IV (Extracellular vesicles group): The major portion of the seminiferous tubules showed an obvious improvement, having an architecture that was approximately normal in appearance. Numerous lines of various germ cells, such as spermatogonia, primary spermatocytes, spermatids, and many spermatozoa filled the lumen. Among some spermatogenic cells tiny vacuoles appeared. Leydig cells were more or less normal (Figure 10).

Group V (Recovery group): Group V exhibited seminiferous tubules with massive disrupted architecture. More or less all germinal epithelium was replaced by large vacuoles leaving few Sertoli &spermatogonia. Interstitial space was filled with abundant inter-tubular amorphous eosinophilic material among numerous blood vessels &abundant Leydig cells (Figure 11).

EM examination

Group I (Control group): Ultrastructural examination of control rat seminiferous tubules revealed Sertoli cells with large, euchromatic nuclei and prominent nucleolus. Type A spermatogonium with its oval nucleus and type B spermatogonium with its rounded nucleus were both encountered. Primary spermatocytes depicted large rounded nuclei. An intact BTB was also noticed. Early spermatids were identified by their pale nuclei with acrosomal vesicle and multiple peripherally situated mitochondria. Multiple spermatozoa were frequently encountered in the lumen of the tubules with their characteristic tails (Figures 12a-f).

Group II (Busulfan group): Ultrastructural inspection of group II revealed spermatogenic cells on irregular basal lamina. Disruption of the normal architecture of the seminiferous tubules was noticed with appearance of large spaces in between the lining cells. Sertoli & spermatogenic cells revealed degenerative changes as abnormal chromatin distribution in their nuclei, cytoplasmic rarefaction, vacuolations and dilated perinuclear cisternae. Mitochondria appeared swollen with focal loss of cristae. The BTB exhibited focal interruptions. In addition to, Middle pieces of tail region were associated with swollen mitochondria & interruptions in the outer dense fibers. (Figures 13 a-f).

Group III (BM-MSCs group): Widening in intercellular spaces was still seen between the spermatogenic cells which showed vacuolated rarefied cytoplasm in certain areas. BTB still exhibited focal interruptions. Alternatively, in other areas normal appearance of spermatogenic cells was observed with mild widening of intercellular space. Some segments in principal pieces showed focal defect in the circumferential ribs (Figures 14a-d).

Group IV (Extracellular vesicles group): Marked improvement in the spermatogenic and Sertoli cells except for few vacuolation present in cytoplasm of SgB. The majority of sperms appeared normal, only few middle

pieces showed focal disruption in mitochondrial sheath and some end pieces exhibited excessive residual cytoplasm (Figures 15a-f).

Group V (Recovery group): Sertoli cells &spermatogenic cells cytoplasm was dense, full of multiple sized vacuoles and rarefaction in several areas. Spermatogonia rested on irregular basal lamina. Dilatation in perinuclear cisternae was seen. Massive ballooning in mitochondrial sheaths of middle pieces were noticed with excessive residual cytoplasm &interrupted outer dense fibers. (Figures 16a-f).

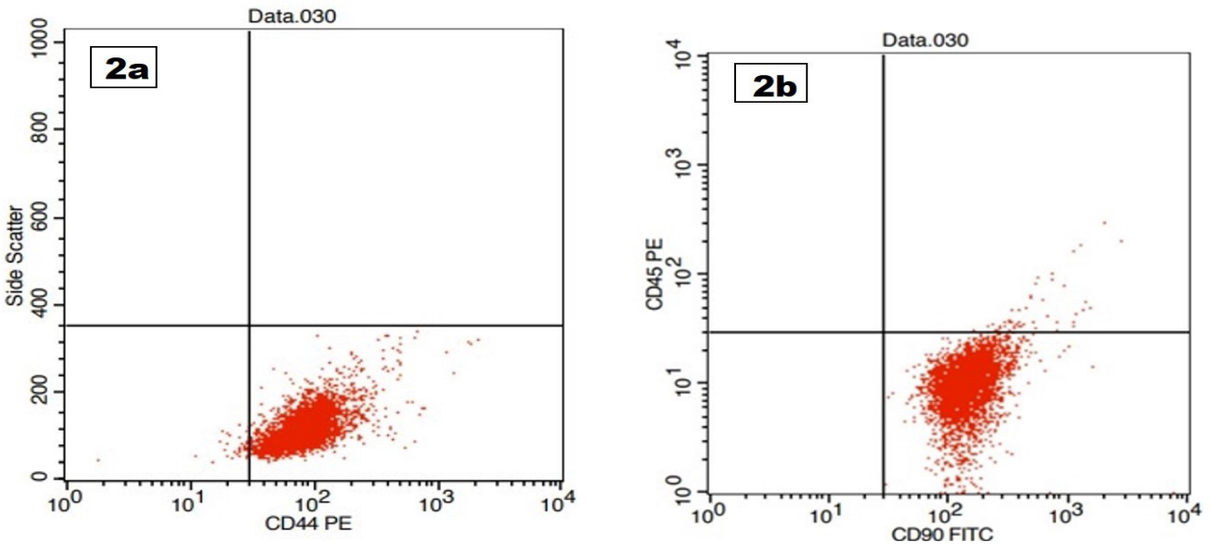

Fig. 2 (a, b): Flow cytometric analysis of cell-surface markers of BM-MSCs at passage3.a) 98.94% of the cultured cells express CD44 in lower right quadrant. b) 98.92% of the cultured cells express CD90 in lower right quadrant, while they are negative for the CD 45 in upper left quadrant.

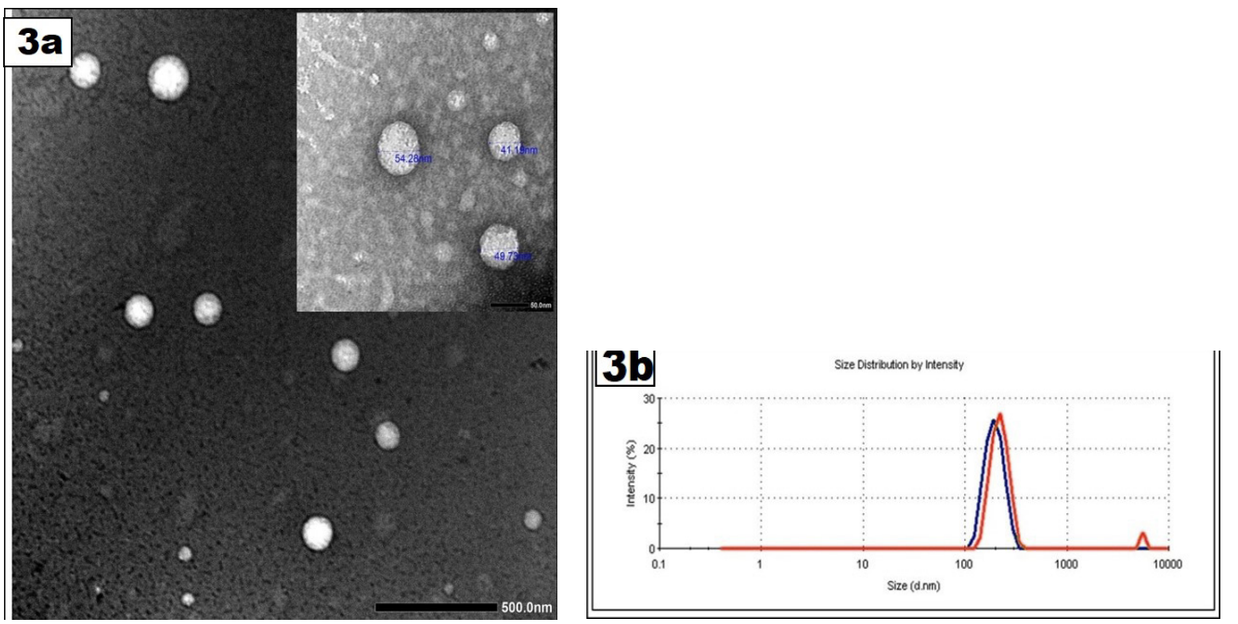

Fig. 3 (a, b): Characterization of EVs: a; TEM of EVs shows variable sized spherical vesicles. Inset: higher magnification of three vesicles surrounded by a double membrane. (Magnification ax15000, inset x100000). b; Size of EVs estimated by zeta sizer nanoparticle analyzer.

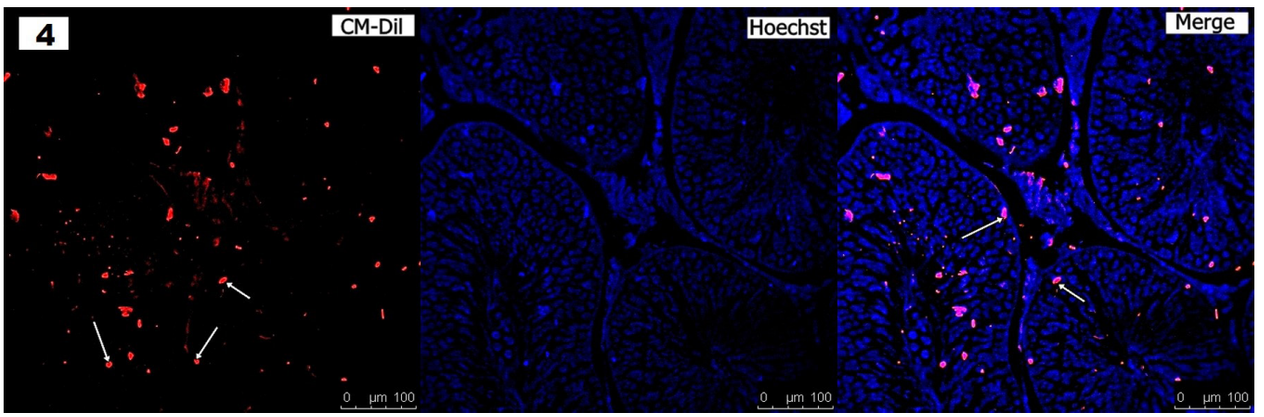

Fig. 4: Photomicrograph of confocal laser microscope of seminiferous tubules showing homed cultured cells expressing red fluorescence of CM-Dil in their cytoplasm (arrows) and nuclei are counterstained in blue with Hoechst stain. (Confocal laser scanning microscope, magnification x 200)

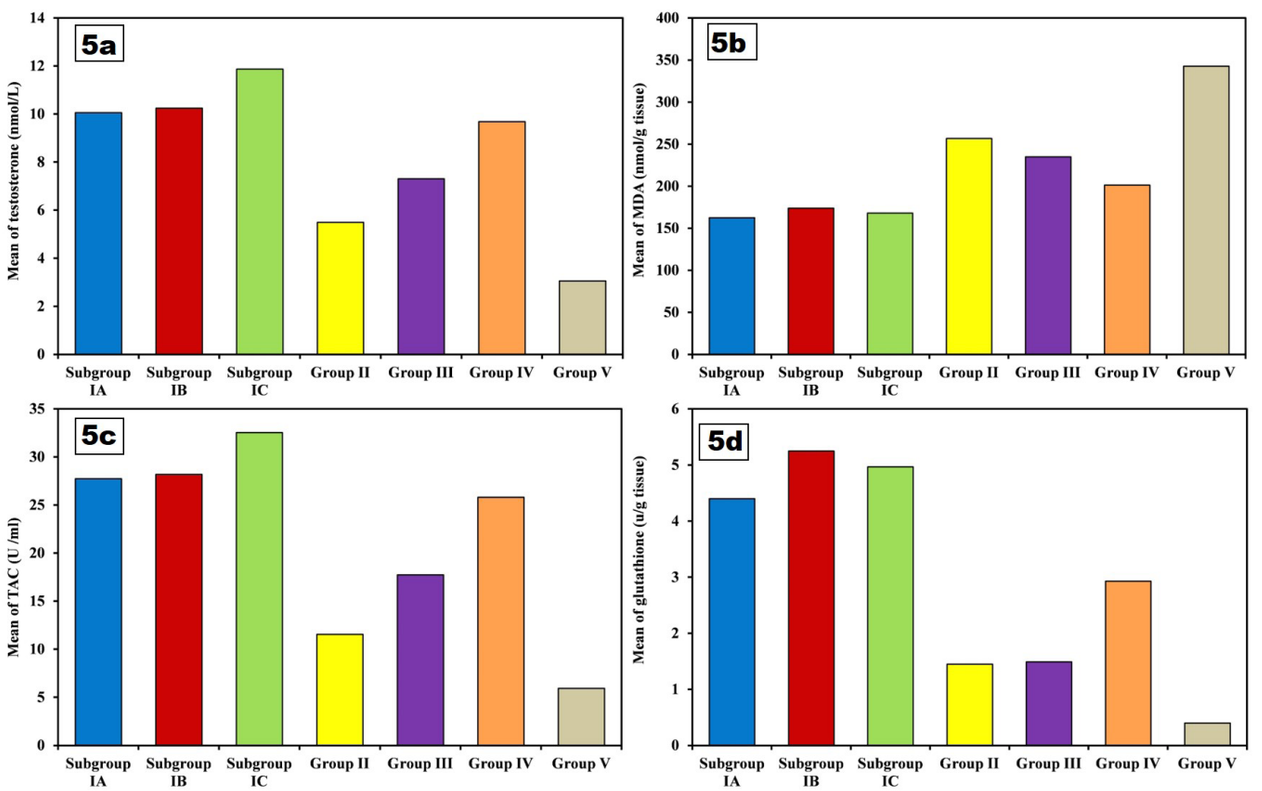

Fig. 5 a-d: Bar charts show mean levels of: a) testosterone in nmol/L, b) MDA in mol//g tissue, c) TAC in U/ml, d) glutathione peroxidase in U/g tissue.

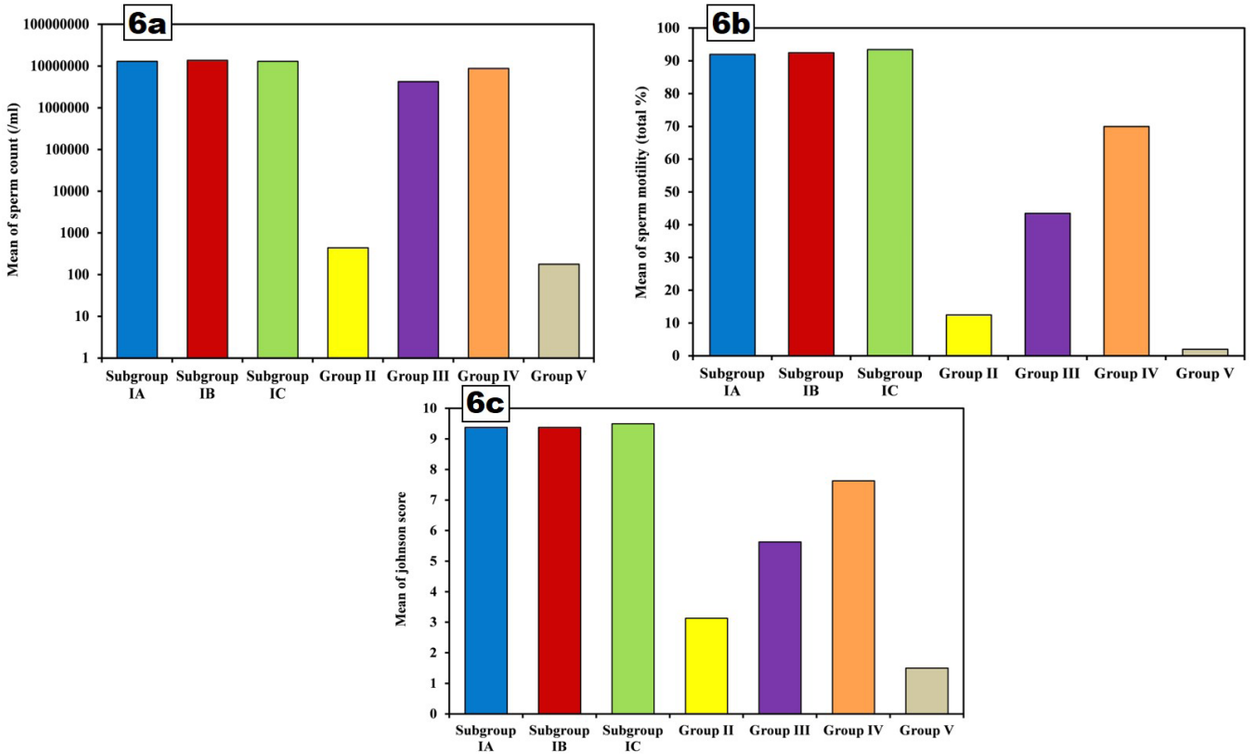

Fig. 6a-c: Bar charts showing comparison between the studied groups according to: a) Sperm count, b) total percentage of sperm motility, c) Johnsen score.

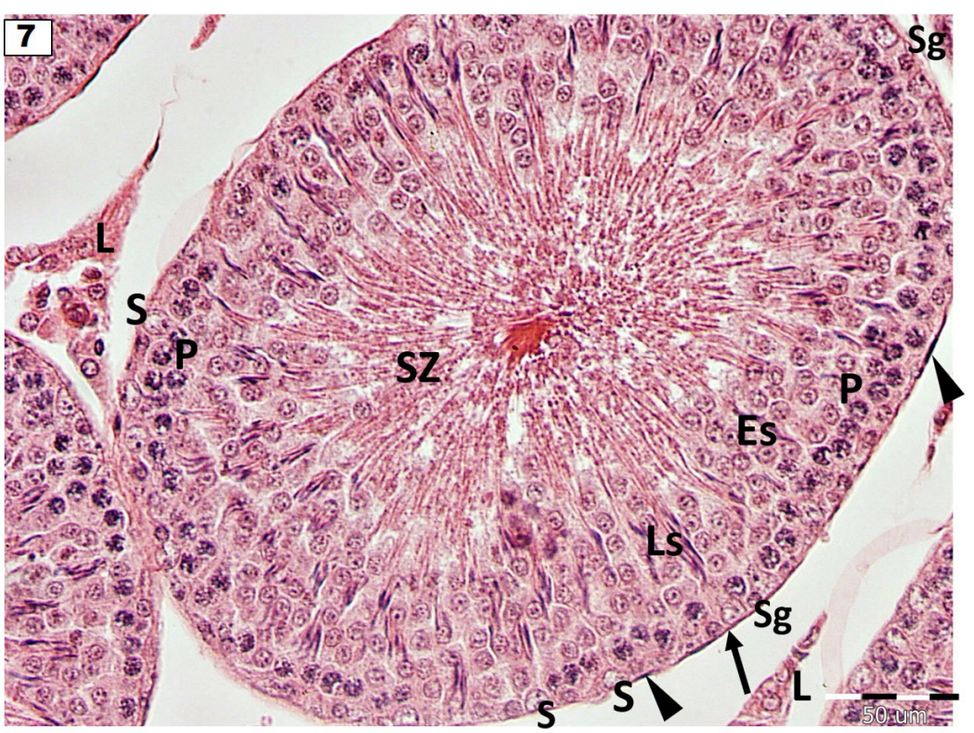

Fig. 7: Light photomicrograph of seminiferous tubule of group I lined by: Sertoli cell (S), Spermatogonia (Sg), primary spermatocytes (P), early spermatids (ES), elongated spermatids (LS) and numerous spermatozoa (SZ) filling the lumen. (↑); basement membrane, (^); myoid cells, L; Leydig cells. (Mag. x 400).

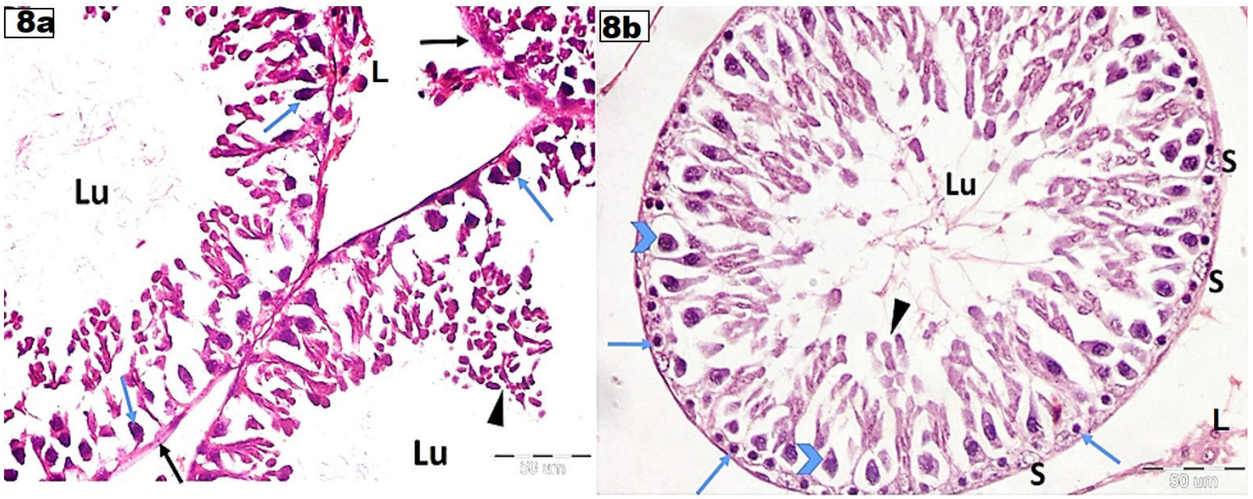

Fig. 8 (a,b): Light photomicrograph of distorted seminiferous tubules of group II showing shrunken spermatogenic cells having deeply stained nuclei (blue arrow) &widened intercellular spaces (chevron arrow). Sertoli cells cytoplasm (S) contain multiple vacuoles. Empty lumen (Lu) with detached spermatogenic cells (^). L; scattered Leydig cell (Mag a, b x 400).

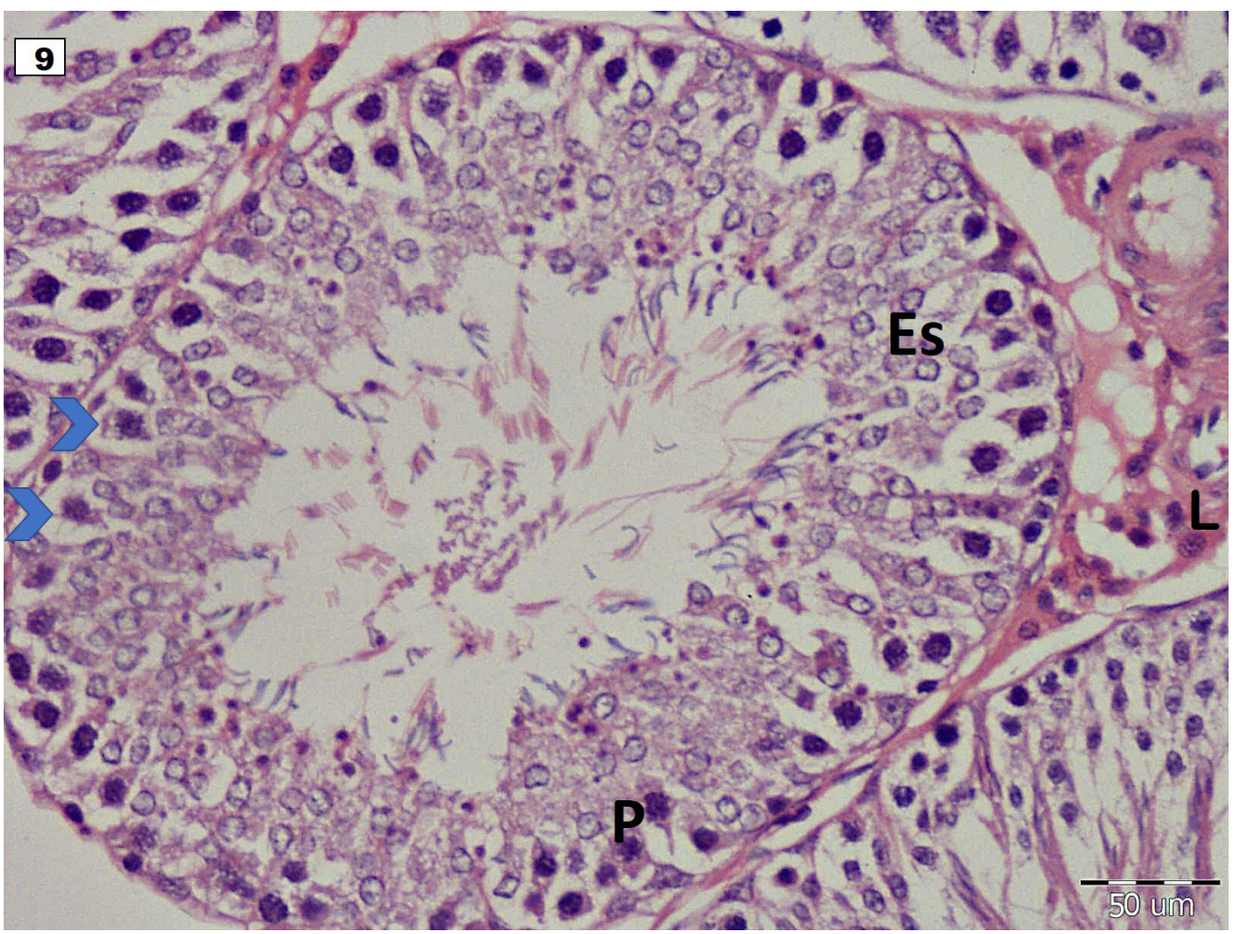

Fig. 9: Light photomicrograph of rat testis of group III revealing shrunken spermatogenic cells with vacuolation in between the cells (chevron arrow). Primary spermatocytes (P) and early spermatids (ES) are seen with widened intercellular spaces. Vacuolations were seen among Leydig cell(L) (Mag. x 400)

Fig. 10: Light photomicrograph of a rat testis of group IV showing seminiferous tubule with organized multiple layers of spermatogenic cells with minute vacuolar spaces in-between (black arrow). Notice multiple sperms (SZ) inside lumen &apparently normal Leydig cells (Mag. x 400).

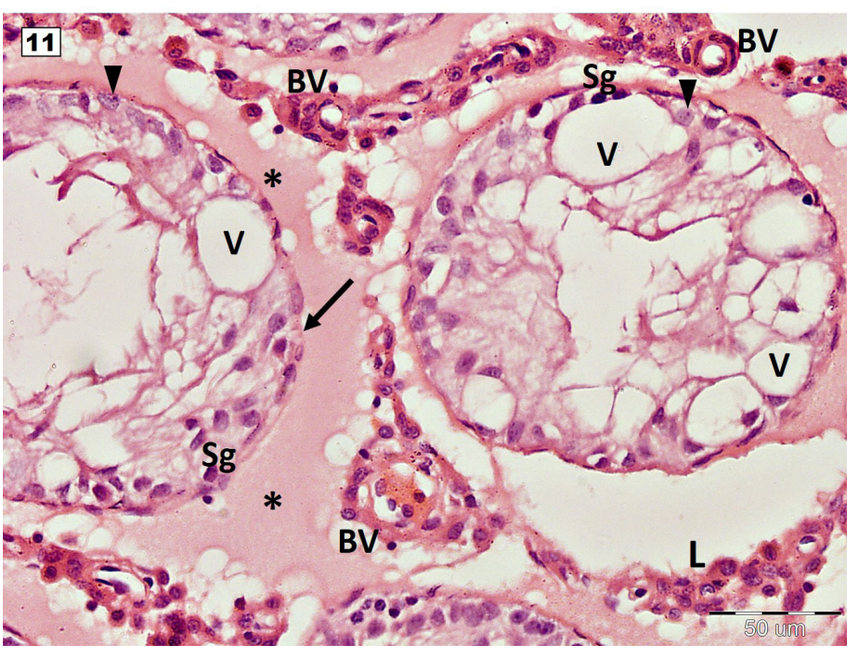

Fig. 11: Light photomicrograph of rat testis of group V, large vacuoles (V) appear within tubular epithelium with nearly total loss of germ cells except few spermatogonia (sg) &few Sertoli cells (^). Amorphous inter-tubular eosinophilic material (*). Apparent increased number of Leydig cells (L) around numerous blood vessels (BV) (Mag. x 400).

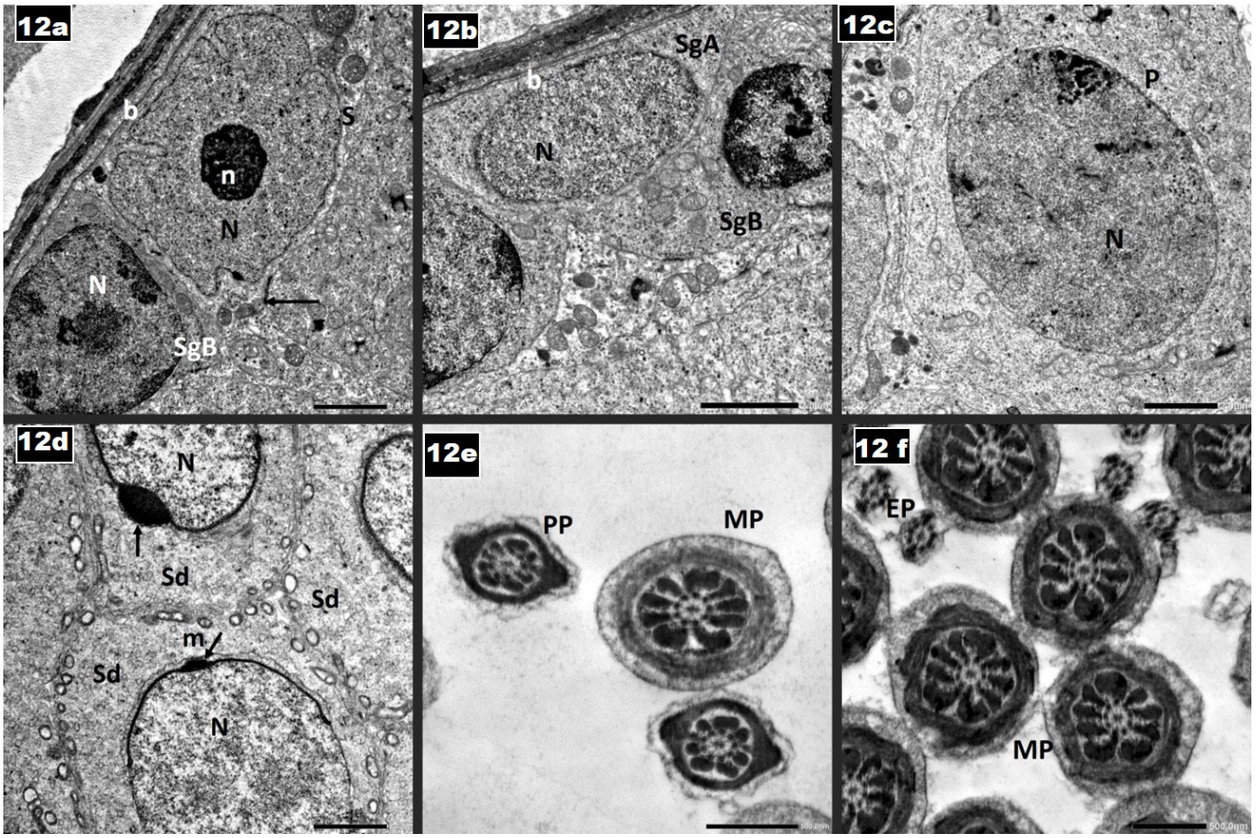

Fig. 12 (a-f): Electron micrographs showing part of seminiferous tubule of group I: a- Sertoli cell (S) with large, pale nucleus (N) and prominent nucleolus (n) resting on basal lamina (b), Type B spermatogonium (SgB) is seen with rounded nucleus (N). Intact blood testis barrier (↑) is detected. b- Type A spermatogonium (SgA) with oval pale nucleus (N).C -Primary spermatocyte with spherical nucleus (N) d- Early spermatids (Sd), with a pale rounded nucleus (N) and acrosomal vesicle (↑). Multiple mitochondria (m) are arranged peripherally. E, f: Multiple cut sections of sperm tails: middle piece (MP), principal piece (PP) and end piece (EP). Mic. Mag. a, c, d x3000, b x4000, e x15000, f x12000.

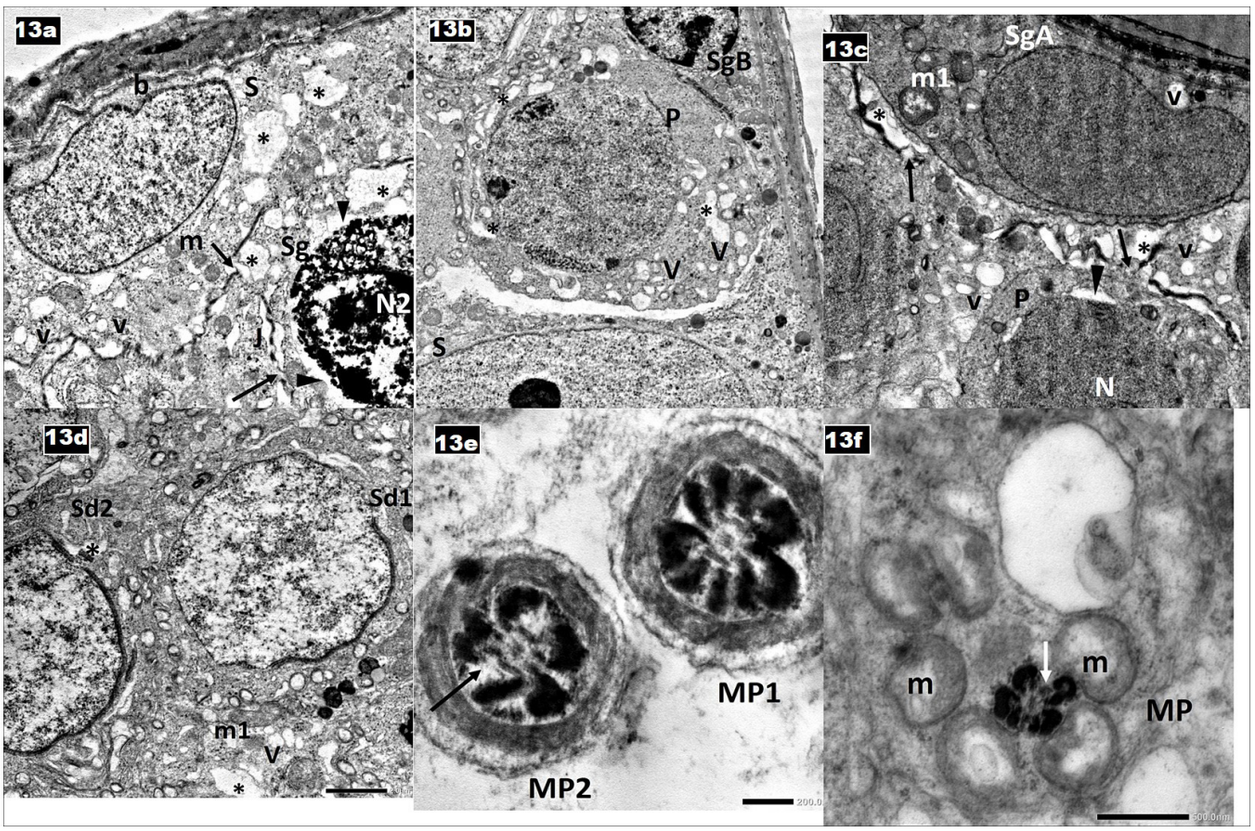

Fig. 13 (a-f): Electron micrographs revealing part of rat seminiferous tubule of group II:a- Sertoli cell (S) resting on irregular basal lamina (b), rarefied cytoplasm (*) and multiple cytoplasmic vacuoles (V). b- Type A spermatogonium (SgA) with mitochondria (m1) showing focal loss of cristae. Disruption of BTB (↑) and widening of intercellular spaces is detected (*).c- Type B spermatogonium (SgB) and primary spermatocyte (P) with vacuoles (V) and rarefaction in its cytoplasm (*). d- Early spermatids (Sd), some mitochondria are swollen (m1). (e,f)-middle piece shows defect & interruptions in the nine outer dense fibers (arrow). Swollen and disorganized mitochondria (m) in mitochondrial sheath. Mic. Mag. a, cx2000, b x3000, dx2500, e x20000, f x15000.

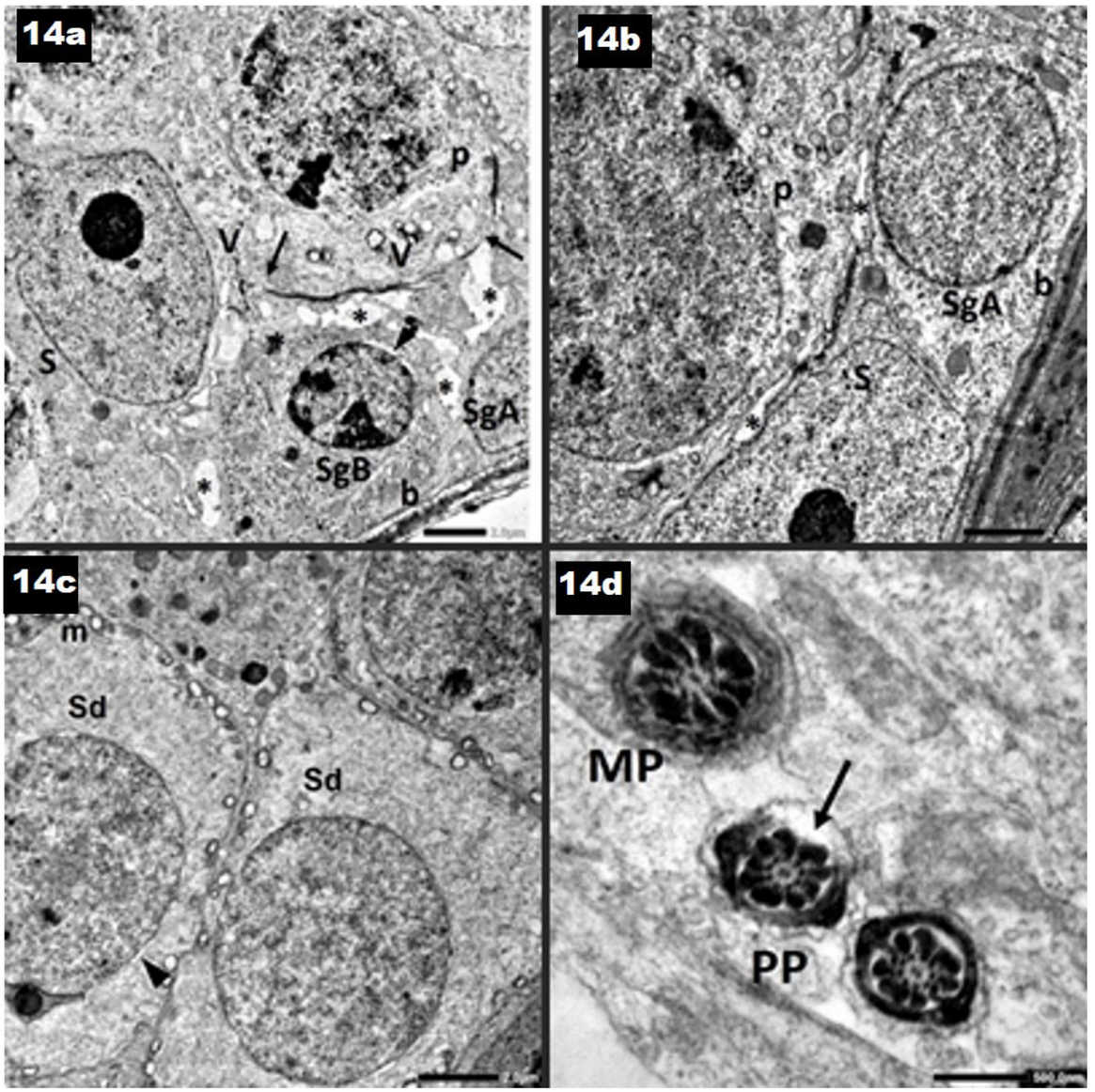

Fig. 14(a-d): Electron micrographs of rat seminiferous tubule of group III: a- type B spermatogonium (SgB) showing apparently normal mitochondria (m). Sertoli cell (S) appears more or less normal. Primary spermatocyte (P) depicts several cytoplasmic vacuoles (V). BTB exhibits focal interruptions (↑). Widening of intercellular spaces is seen (*). b- Type A spermatogonium (SgA) &Primary spermatocyte (P) seen with mild intercellular spaces (*). c- Early spermatids (Sd) surrounded by slightly focal dilated perinuclear cisternae ( ). d-Principal piece depicts focal interruption (arrow) of the circumferential ribs. Mic. mag ax2000, b, c x2500, d x 20000.

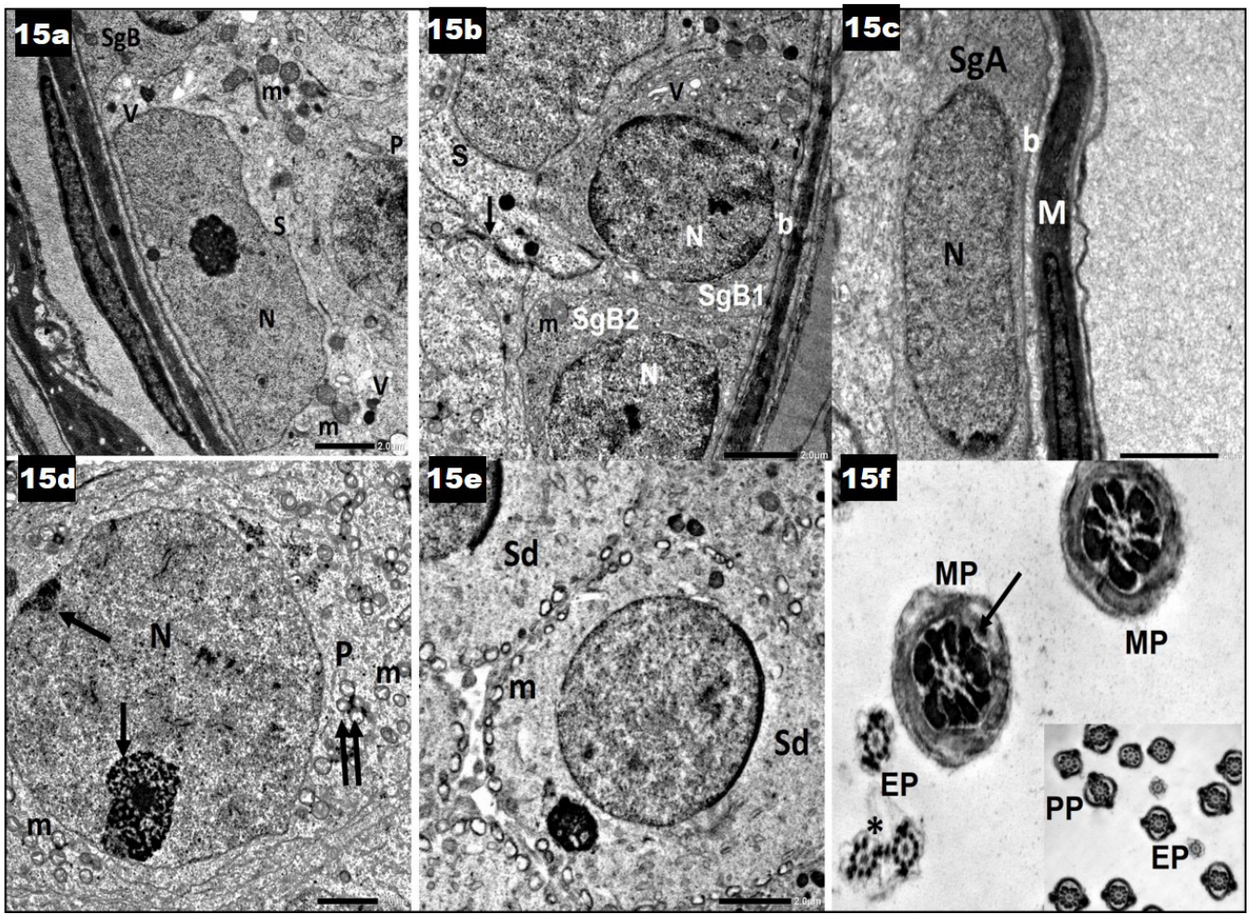

Fig. 15(a-f): Electron micrographs of rat seminiferous tubule of group IV: a- Sertoli cell (S) with pale nucleus (N). b- two adjacent type B spermatogonia (SgB) resting on a basal lamina (b). The cytoplasm in SgB1 shows mild vacuolation(V). Focal interruption (↑) in BTB is noticed. c,d-,e: apparently normal type A spermatogonium (SgA),spermatids(sd), primary spermatocyte (P) cytoplasm exhibits mitochondria (m),few show disrupted cristae (↑↑). f-Middle piece (MP) exhibits focal disruption (↑) in mitochondrial sheath and end piece (EP) exhibit excess residual cytoplasm (*). Inset, cross sections of normal principal pieces (PP) and end pieces (EP) Mic. mag a, dx2500, b, e x3000, c x4000, f & inset x12000.

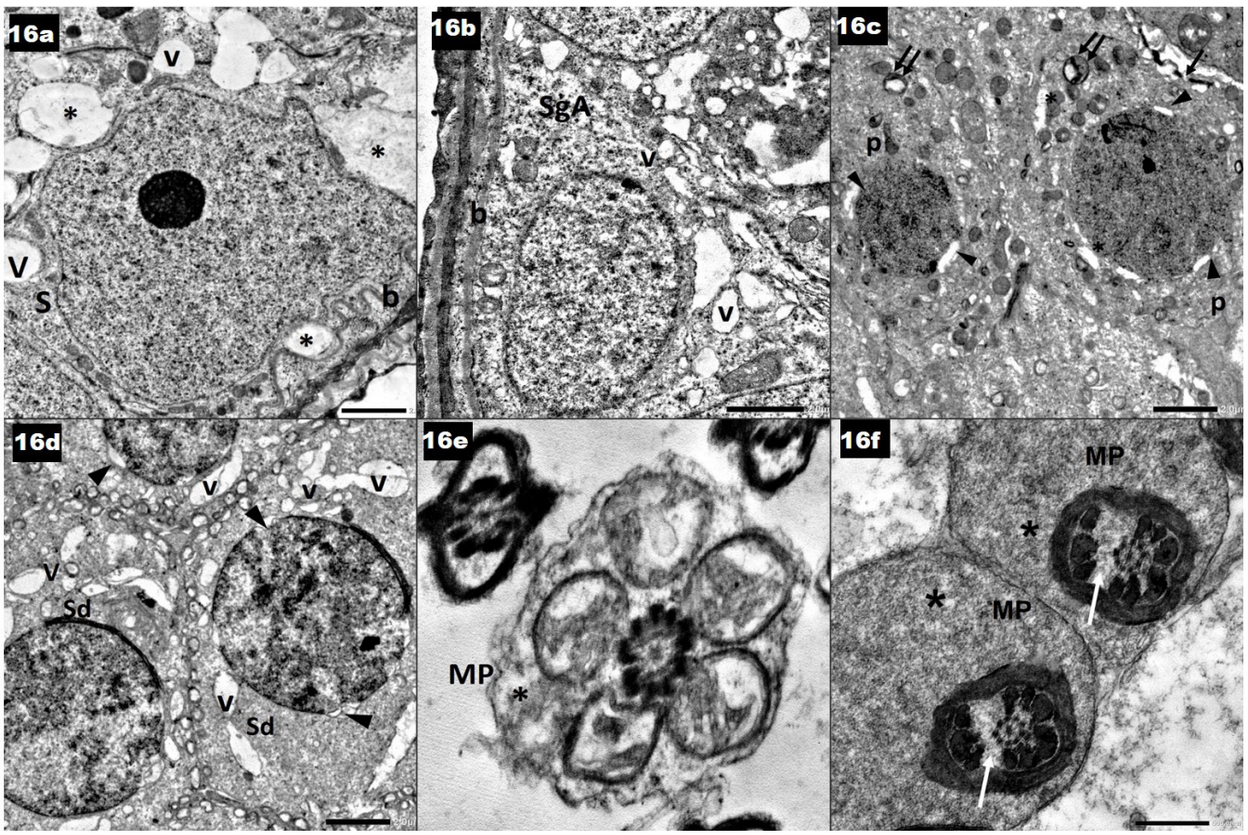

Fig. 16(a-f): Electron micrographs of rat seminiferous tubule of group V: a- revealing Sertoli cell (S) resting on irregular basal lamina (b). Its cytoplasm exhibits multiple vacuoles(V)and rarefaction (*).b- spermatogonium type A (SgA) with vacuoles(V) c-2 adjacent primary spermatocytes (P) with dilated perinuclear cisterna ( ) and rarefied cytoplasm (*). mitochondria with focal loss of cristae (↑↑), disrupted BTB (↑). d- early spermatids (Sd) cytoplasm full of vacuoles (V) .e- middle pieces (MP) of sperm tail with massive ballooning in mitochondrial sheath and excess residual cytoplasm is noticed (*). f-MP depicts focal interruptions (arrow) in the nine outer dense fibers and excessive residual cytoplasm (*) Mag. a, cx2500 b x3000, dx2000, e x20000, f x12000.

DISCUSSION

One major issue affecting reproductive health worldwide is infertility half of the cases involve a male factor[34]. The most problematic long-term side effect of cancer treatment is testicular dysfunction following chemotherapy[35]. Patients with chronic and juvenile myelogenous leukemia receive busulfan (BU) as part of their conditioning regimen prior to hematopoietic cell transplantation (HCT)[36]. In addition to its gonadotoxic effects, alterations in sperms number& hormonal levels leading to diminished testicular size, and ultimately male infertility[37,38].

Each rat in the current study was injected once intraperitoneally with 40 mg/kg body weight BU. It has been established by previous researches[22,38] that this dose effectively inhibits spermatogenesis, &lowers testosterone levels after a single injection. The 50 mg/kg dosage of BU was reported to be deadly by Wang *et al*.[39] most likely as a result of the hematopoietic system's cytotoxic reactions to the medication. After 28 days of BU administration, light microscopic examination of group II (BU group), revealed distorted seminiferous tubules. Spermatogenic cells& Sertoli cells displayed signs of degeneration. These findings were in accordance with several studies investigating the effect of BU induced testicular injury[40,41].

BU has the capability to alkylate DNA at guanine & adenine bases, leading to the formation of intra-strand crosslinks. As a consequence, hinders transcription of DNA, ultimately impeding cellular division. Busulfan also initiates the extrinsic apoptotic pathway and triggers execution caspases 3, 7&8. Caspase 3 controls DNA fragmentation and morphologic changes of apoptosis & Caspase-7, is responsible for ROS production &aids in cell detachment during apoptosis[42]. BU treatment induced ferroptosis in spermatogenic cells by down-regulating nuclear factor-E2-related factor 2 (Nrf2) and glutathione peroxidase 4 (GPX4) expressions, and decreasing iron efflux through reduction of ferroportin 1 (FPN1) expression[43]. This could clarify the histological changes observed attributed to busulfan-induced ferroptosis such as dark pyknotic nuclei in spermatogenic cells with increased intercellular spaces, disruption of mitochondria[43,44]. Furthermore, the rapid cell division rate and the prevalence of unsaturated fatty acids make male germ cells prone to DNA deterioration[45].

Vacuolations observed within Sertoli cells represents dilatation in smooth endoplasmic reticulum (sER). Possible mechanisms include alterations in secretion or transport of proteins out of the sER, disruption of sER ionic pumps,

or changes in the cytoskeleton supporting the sER. TEM findings of enlarged mitochondria, dilated perinuclear cisternae around spermatogenic cells and vacuolated rarefied cytoplasm were due to lipid peroxidation and oxidative stress induced by BU[38,46].

Moreover, the expression of intercellular adhesion molecule-1 (ICAM-1), that directs the discharge of spermatids to the lumen is also significantly reduced by BU.[47,48]. According to Jiang *et al*.[49], BU causes disruptions to the blood testes barrier(BTB) and hinders the process of sperm formation by increasing the level of non-collagenous 1 domain peptide (NC1) .These could provide an explanation for the BTB disrupted junctional complex. Additionally, it was discovered that busulfan administration activated the production of proteins such tumour necrosis factor-α and macrophage chemotactic protein 1, which caused inflammation in the mice's testes[50].

In the current study, serum and tissue homogenates of rats injected with busulfan showed a substantial increase in the oxidant marker MDA together with a sharp decline in antioxidants total TAC and glutathione peroxidase). Together with a decline in sperm parameters, the Johnsen score, and serum testosterone. This dramatic decrease in hormone testosterone may be related to the significant damage busulfan caused to Leydig and Sertoli cells, possibly as a result of increased production of free radicals. Additionally, disruption of the Luteinizing Hormone (LH) receptor's production and suppression of the passage of cholesterol to cytochrome P-450 of the mitochondria affecting the initial steps in testosterone production[51].

The stimulation of oxidative stress and lipid peroxidation can be used to explain the reduction in sperm quantity and total percentage of motility reported in this study. Because sperm plasma membranes have a high concentration of unsaturated fatty acids and weak antioxidant defenses, they are especially susceptible to oxidative damage[52].

Rats of group III which were injected by BM-MSCs showed partial improvement detected by both biochemical profile and microscopic examinations. These findings were confirmed by improvements in the epididymal sperm count, Johnson score and hormonal levels of testosterone in comparison with the busulfan group. In the current study, the steps of isolation, culture and passaging of BM-MSCs were adopted with several previous studies Moussa *et al* and Rostom *et al*[19,53].

Because the large diameter of stem cells (20–30 μm), worries regarding cell entrapment in the lungs led to the exclusion of the systemic intravenous route for the injection[54]. Furthermore, physiological BTB prevent MSCs from penetrating testes[55,56]. The decision made was to inject cells into the efferent ducts instead. BM-MSCs are simple to harvest and exhibit minimal immune suppression and rejection rates[57]. That's why BM-MSCs were used in this study.

LM &ultrastructure of group III (BU+BM-MSCs) depicted seminiferous tubules with varying response to treatment, partial enhancement in spermatogenic cells was detected in comparison to BU group. Some tubules depicted developing spermatogenic cells with spermatozoa in their lumina. These findings align with studies by Monsefi *et al*.[58] &Tamadon *et al*.[59] reported the transition from stem cells to spermatogenic cells and spermatozoa in *vitro*, as transforming growth factor beta (TGF-β) and bone morphogenetic proteins (BMPs) discharged by the transplanted cells can aid in the recipient's cellular function recovering back to normal. However, contrary results were presented by Van Saen *et al*.[60] declaring that BM-MSCs were incapable of differentiating into sperm.

The results of the current study confirmed that BM-MSCs administration enhanced testosterone levels, which is consistent with Hassen *et al*.[61] Remarkably, another study verified MSCs' capacity to develop into Leydig cells[62].

Additionally, by boosting the expression of anti-oxidant enzymes including glutathione (GSH) and glutathione S-transferase (GST), which capture reactive oxygen species secreting factors that block the oxidation process, such as prostaglandin E2 and nitric oxide, stem cells alleviate oxidative-stress[63]. By inhibiting ROS, the cells enhance oxidative stress injury, according to Zickri *et al*.[64] TNF-α is a major factor that BM-MSCs use to actively participate in anti-inflammatory actions by lowering its level.These could explain noteworthy reduction in tissue MDA level and great surge in serum TAC and tissue glutathione peroxidase level, enhanced total sperm number and total percentage of sperm motility in the stem cells' treated group if compared to the rats given BU.

However, a number of obstacles restrict using BM-MSCs as cells numbers and proliferative potential noticeably decline with age[65]. In proportion to this issue, an alternative option is proposed utilizing the paracrine pathway such as exosomes.

Histological examination of group IV (BU+BM derived extracellular vesicles) revealed massive improvement in most of the seminiferous tubules with regaining normal architecture. Secretory factors from EVs were found to successfully delay spermatogenesis in busulfan-induced rats in a study conducted by Cai *et al*.[66] Spermatogonia were shown to be able to internalize exosomes from bone marrow mesenchymal stem cells as demonstrated by Guo *et al*.[67].

One of the mechanisms by which EVs can restore spermatogenesis is their ability to cross the BTB delivering their cargos. Following the injection of labelled stem cell-derived EVs into the rat efferent duct, their presence was detected in both seminiferous tubules and the interstitial space. This finding suggests that EVs have the capability to traverse the BTB, moving from seminiferous tubules to the interstitium[68]. According to Zhou *et al*.[69], BM-derived exosomes can improve BTB function in ageing testes by

strengthening the tight junction function &reducing ROS generation .All of these account for the improvement in group IV's BTB configuration.

One of the fundamental cargoes of BM-MSCs-EVs is miRNAs. miR-34 family members (miR-34b and miR-34c) control apoptosis and the differentiation of cells. Exosomes generated from Sertoli cells express miR-486 to support further differentiation of spermatogonia[71]. Moreover, miR-223 and miR-124-3p present in BM-MSCs-EVs have the capability to induce anti-inflammatory effects. This is achieved by downregulating proinflammatory mediators and adhesion molecules, including IL-6, TNF-α and ICAM-1[70,72].

Biochemical tests of group IV (BM-MSCs -EVs) revealed significant elevation of testosterone levels &TAC level was noticed, together with significant reduction in mean values of glutathione peroxidase and MDA. A study demonstrated exosomes augmented the activity of superoxide dismutase (SOD) in testicular tissue subjected to ischemia-reperfusion injury. Additionally, there was a reduction in the content of MDA, indicating a potential antioxidative effect of extracellular vesicles secreted from BM-MSCs in the treated testicular tissue[73]. Sperm count and motility were greatly improved in group IV as EVs transport several cytokines and factors to spermatozoa, such as sorbitol dehydrogenase and macrophage migration inhibitory factor. By activating cation channels of sperms and the acrosome reaction, this process increases Ca2+ signaling and improves integrity of sperm membrane[74].

In group V, where rats were left for spontaneous recovery, the seminiferous tubules exhibited similar degenerative changes to group II, with massive exacerbation. The inability of autonomous tubular regeneration following BU administration has similarly been documented by Ibrahim *et al*.[22]. This restricted regeneration may be explained by spermatogonial stem cells' inability to multiply and differentiate in the unfavorable environment created by chemotherapy. On the other hand, another study found that the amount and duration of exposure to busulfan affect germ cell recovery. High doses of chemotherapy may cause the seminiferous tubules to completely deplete, leaving a patient permanently sterile. Alternatively, germ cell recovery may be possible at lower busulfan dosages, suggesting a reversible impact on spermatogenesis[75].

Significant inter-tubular eosinophilic material was found in groups II and V. This observation may have been affected by busulfan's ability to up-regulate in Sertoli cells TNF-α and monocyte chemoattractant protein-1 (MCP-1). Furthermore, it has been suggested that nuclear factor-kappa beta (NF-κβ) signaling pathway is triggered by reactive oxygen species, hence increasing the transcription of many genes that are associated with inflammation[27].

All of these elements combined created inflammatory state in the testis, which interfered with the testicular venous drainage system, lymphatic vessels blockage and resulted in massive appearance of eosinophilic material and congested vessels in between the tubules.The increased number of Leydig cells &interstitial blood vessels observed in this experimental group further indicated inflammatory& oxidative stress processes[76].

Johnsen's score evaluation system has been widely utilized in various studies to assess testicular histopathology. This system provides a comprehensive grading system, assigning scores from 10 to 1 based on the degree of spermatogenesis within the testicular tubules. A lower score is associated with a reduction in the quantity of cells in the tubule lumen. Several studies have demonstrated the utility of Johnsen's score[77,78]. In the context of our study, we employed Johnsen's criteria to evaluate rats' testicular histopathology following exposure to BU. Our results indicated a significant reduction in Johnsen's score in the BU and recovery groups in comparison to the first group and elevated Johnson score after administration of BM-MSCs and EVs highlighting the beneficial effects of them on improving testicular injury.

CONCLUSION

EVs as a cell-free therapy present a novel and promising approach in the treatment of busulfan induced testicular injury showing better results & several advantages such as miRNAs cargo and beneficial growth factors and cytokine production over traditional MSC transplantation

CONFLICT OF INTERESTS

There are no conflicts of interest

REFERENCES

1. Botezatu A, Vladoiu S, Fudulu A, Albulescu A, Plesa A, Muresan A, *et al*. Advanced molecular approaches in male infertility diagnosis†. Biol Reprod 2022;107(3):684-704. DOI:10.1093/biolre/ioac105.
2. Yumura Y, Takeshima T, Komeya M, Karibe J, Kuroda S, Saito T. Long-Term Fertility Function Sequelae in Young Male Cancer Sur*vivo*rs. World J Mens Health 2023;41(2):255-71. DOI:10.5534/wjmh.220102.
3. Delessard M, Saulnier J, Rives A, Dumont L, Rondanino C, Rives N. Exposure to Chemotherapy During Childhood or Adulthood and Consequences on Spermatogenesis and Male Fertility. Int J Mol Sci 2020;21(4). DOI:10.3390/ijms21041454.
4. Lüftinger R, Zubarovskaya N, Galimard JE, Cseh A, Salzer E, Locatelli F, *et al*. Busulfan-fludarabine- or treosulfan-fludarabine-based myeloablative conditioning for children with thalassemia major. Ann Hematol 2022;101(3):655-65. DOI:10.1007/s00277-021-04732-4.
5. Puyo S, Montaudon D, Pourquier P. From old alkylating agents to new minor groove binders. Crit Rev Oncol Hematol 2014;89(1):43-61. DOI:10.1016/j.critrevonc.2013.07.006.

6. Szydlak R. Biological, chemical and mechanical factors regulating migration and homing of mesenchymal stem cells. World J Stem Cells 2021;13(6):619-31. DOI:10.4252/wjsc.v13.i6.619.

7. Zhou T, Yuan Z, Weng J, Pei D, Du X, He C, *et al*. Challenges and advances in clinical applications of mesenchymal stromal cells. J Hematol Oncol 2021;14(1):24. DOI:10.1186/s13045-021-01037-x.

8. Erwin N, Serafim MF, He M. Enhancing the Cellular Production of Extracellular Vesicles for Developing Therapeutic Applications. Pharm Res 2023;40(4):833-53. DOI:10.1007/s11095-022-03420-w.

9. Buratta S, Urbanelli L, Tognoloni A, Latella R, Cerrotti G, Emiliani C, *et al*. Protein and Lipid Content of Milk Extracellular Vesicles: A Comparative Overview. Life 2023;13(2):401. DOI:10.3390/life13020401.

10. Jurj A, Zanoaga O, Braicu C, Lazar V, Tomuleasa C, Irimie A, *et al*. A Comprehensive Picture of Extracellular Vesicles and Their Contents. Molecular Transfer to Cancer Cells. Cancers (Basel) 2020;12(2). DOI:10.3390/cancers12020298.

11. Matsuzaka Y, Yashiro R. Therapeutic Strategy of Mesenchymal-Stem-Cell-Derived Extracellular Vesicles as Regenerative Medicine. Int J Mol Sci 2022;23(12). DOI:10.3390/ijms23126480.

12. Kumar MA, Baba SK, Sadida HQ, Marzooqi SA, Jerobin J, Altemani FH, *et al*. Extracellular vesicles as tools and targets in therapy for diseases. Signal Transduct Target Ther 2024;9(1):27. DOI:10.1038/s41392-024-01735-1.

13. Kodam SP, Ullah M. Diagnostic and Therapeutic Potential of Extracellular Vesicles. Technol Cancer Res Treat 2021;20:15330338211041203. DOI:10.1177/15330338211041203.

14. Zakaria DM, Zahran NM, Arafa SAA, Mehanna RA, Abdel-Moneim RA. Histological and Physiological Studies of the Effect of Bone Marrow-Derived Mesenchymal Stem Cells on Bleomycin Induced Lung Fibrosis in Adult Albino Rats. Tissue Eng Regen Med 2021;18(1):127-41. DOI:10.1007/s13770-020-00294-0.

15. Freitas GP, Souza ATP, Lopes HB, Trevisan RLB, Oliveira FS, Fernandes RR, *et al*. Mesenchymal Stromal Cells Derived from Bone Marrow and Adipose Tissue: Isolation, Culture, Characterization and Differentiation. Bio Protoc 2020;10(4):e3534. DOI:10.21769/BioProtoc.3534.

16. Li W, Zeng J, Zhu G, Dong Y, Xie D, Lai R. In *Vitro* Cultivation Technology of Rat Bone Marrow Mesenchymal Stem Cells. J Biomater Tissue Eng 2019;9:62-8. DOI:10.1166/jbt.2019.1946.

17. Penfornis P, Pochampally R. Colony Forming Unit Assays. Methods Mol Biol 2016;1416:159-69. DOI:10.1007/978-1-4939-3584-0_9.

18. Khan MR, Chandrashekran A, Smith RK, Dudhia J. Immunophenotypic characterization of ovine mesenchymal stem cells. Cytometry A 2016;89(5):443-50. DOI:10.1002/cyto.a.22849.

19. Rostom DM, Attia N, Khalifa HM, Abou Nazel MW, El Sabaawy EA. The Therapeutic Potential of Extracellular Vesicles Versus Mesenchymal Stem Cells in Liver Damage. Tissue Eng Regen Med 2020;17(4):537-52. DOI:10.1007/s13770-020-00267-3.

20. Woo CH, Kim HK, Jung GY, Jung YJ, Lee KS, Yun YE, *et al*. Small extracellular vesicles from human adipose-derived stem cells attenuate cartilage degeneration. J Extracell Vesicles 2020;9(1):1735249. DOI:10.1080/20013078.2020.1735249.

21. González-Cubero E, González-Fernández ML, Gutiérrez-Velasco L, Navarro-Ramírez E, Villar-Suárez V. Isolation and characterization of exosomes from adipose tissue-derived mesenchymal stem cells. J Anat 2021;238(5):1203-17. DOI:10.1111/joa.13365.

22. Ibrahim HF, Safwat SH, Zeitoun TM, El Mulla KF, Medwar AY. The Therapeutic Potential of Amniotic Fluid-Derived Stem Cells on Busulfan-Induced Azoospermia in Adult Rats. Tissue Eng Regen Med 2021;18(2):279-95. DOI:10.1007/s13770-020-00309-w.

23. Mobarak H, Heidarpour M, Rahbarghazi R, Nouri M, Mahdipour M. Amniotic fluid-derived exosomes improved spermatogenesis in a rat model of azoospermia. Life Sci 2021;274:119336. DOI:10.1016/j.lfs.2021.119336.

24. Jalalie L, Rezaie MJ, Jalili A, Rezaee MA, Vahabzadeh Z, Rahmani MR, *et al*. Distribution of the CM-Dil-Labeled Human Umbilical Cord Vein Mesenchymal Stem Cells Migrated to the Cyclophosphamide-Injured Ovaries in C57BL/6 Mice. Iran Biomed J 2019;23(3):200-8. DOI:10.29252/.23.3.200.

25. Gill ME, Kohler H, Peters A. Dual DNA staining enables isolation of multiple sub-types of post-replicative mouse male germ cells. Cytometry A 2022;101(6):529-36. DOI:10.1002/cyto.a.24539.

26. Rostami A, Vakili S, Koohpeyma F, Jahromi BN, Aghajari ZA, Mahmoudikohani F, *et al*. Ellagic acid effects on testis, sex hormones, oxidative stress, and apoptosis in the relative sterility rat model following busulfan administration. BMC Complement Med Ther 2022;22(1):170. DOI:10.1186/s12906-022-03650-w.

27. Abarikwu SO, Njoku RC, John IG, Amadi BA, Mgbudom-Okah CJ, Onuah CL. Antioxidant and anti-inflammatory protective effects of rutin and kolaviron against busulfan-induced testicular injuries in rats. Syst Biol Reprod Med 2022;68(2):151-61. DOI:10.1080/19396368.2021.1989727.

28. Koracevic D, Koracevic G, Djordjevic V, Andrejevic S, Cosic V. Method for the measurement of antioxidant activity in human fluids. J Clin Pathol 2001;54(5):356-61. DOI:10.1136/jcp.54.5.356.

29. Abougalala FMA, Ali EK, Fayyad RMA, Elsaied MY, Abdelmonsef AS. Mesenchymal stem cells for Busulfan–Induced Azoospermia: An experimental study. Int J Med Arts 2022;4(4):2319-24. DOI:10.21608/IJMA.2022.237915.

30. Ghorbanlou M, Rostamkhani S, Shokri S, Mahmazi S, Fallah R, Moradi F, *et al*. Possible ameliorating effects of Glycyrrhiza Glabra (Licorice) on the sperm parameters in rats under high fat diet. Endocr Regul 2020;54(1):22-30. DOI:10.2478/enr-2020-0004.

31. Bilinska B, Hejmej A, Kotula-Balak M. Preparation of Testicular Samples for Histology and Immunohistochemistry. Methods Mol Biol 2018;1748:17-36. DOI:10.1007/978-1-4939-7698-0_3.

32. Teixeira TA, Pariz JR, Dutra RT, Saldiva PH, Costa E, Hallak J. Cut-off values of the Johnsen score and Copenhagen index as histopathological prognostic factors for postoperative semen quality in selected infertile patients undergoing microsurgical correction of bilateral subclinical varicocele. Transl Androl Urol 2019;8(4):346-55. DOI:10.21037/tau.2019.06.23.

33. Kuo J. Electron microscopy: methods and protocols. 2nd ed. New Jersy: Humana Press Inc; 2007.

34. Gül M, Russo GI, Kandil H, Boitrelle F, Saleh R, Chung E, *et al*. Male Infertility: New Developments, Current Challenges, and Future Directions. World J Mens Health 2024;2:230232. DOI:10.5534/wjmh.230232.

35. Ibrahim HG, Zoheir MA, Hashem FE, Zewail M, Abd-el-Moneim RA. Histological and Biochemical Evaluation of the Possible Protective Effect of Thymoquinone Loaded Nanostructured Lipid Carriers Versus Thymoquinone on Cisplatin Induced Testicular Toxicity in Adult Rats. Egypt J Histol. 2023 Dec 1;46(4):1911-33. DOI: 10.21608/EJH.2022.161298.1770

36. Sakashita K, Yoshida N, Muramatsu H, Ohtsuka Y, Watanabe K, Yabe M, *et al*. Allogeneic Hematopoietic Cell Transplantation for Juvenile Myelomonocytic Leukemia with a Busulfan, Fludarabine, and Melphalan Regimen: JPLSG JMML-11. Transplant Cell Ther 2024;30(1):105.e1-.e10. DOI:10.1016/j.jtct.2023.10.002.

37. Faraci M, Diesch T, Labopin M, Dalissier A, Lankester A, Gennery A, *et al*. Gonadal Function after Busulfan Compared with Treosulfan in Children and Adolescents Undergoing Allogeneic Hematopoietic Stem Cell Transplant. Biol Blood Marrow Transplant 2019;25(9):1786-91. DOI:10.1016/j.bbmt.2019.05.005.

38. Abd El-Hay RI, Hamed WHE, Mostafa Omar N, Refat El-Bassouny D, Gawish SA. The impact of busulfan on the testicular structure in prepubertal rats: A histological, ultrastructural and immunohistochemical study. Ultrastruct Pathol 2023;47(5):424-50. DOI:10.1080/01913123.2023.2234470.

39. Wang DZ, Zhou XH, Yuan YL, Zheng XM. Optimal dose of busulfan for depleting testicular germ cells of recipient mice before spermatogonial transplantation. Asian J Androl 2010;12(2):263-70. DOI:10.1038/aja.2009.67.

40. Kim KH, Park MJ, Park NC, Park HJ. Effect of N-acetyl-L-cysteine on Testicular Tissue in Busulfan-Induced Dysfunction in the Male Reproductive System. World J Mens Health 2023;41(4):882-91. DOI:10.5534/wjmh.220100.

41. Ezim O, Abarikwu S. Exogenous Ascorbate Administration Elevates Testicular Oxidative Damage and Histological Injuries in Rats after Busulfan Treatment. Andrologia 2023;2023:1-10. DOI:10.1155/2023/5209480.

42. Brentnall M, Rodriguez-Menocal L, De Guevara RL, Cepero E, Boise LH. Caspase-9, caspase-3 and caspase-7 have distinct roles during intrinsic apoptosis. BMC cell biology. 2013 Dec;14:1-9. DOI: 10.1186/1471-2121-14-32

43. Zhao X, Liu Z, Gao J, Li H, Wang X, Li Y, Sun F. Inhibition of ferroptosis attenuates busulfan-induced oligospermia in mice. Toxicology. 2020 Jul 1;440:152489. DOI:10.1016/j.tox.2020.152489.

44. Ganjalikhan Hakemi S, Sharififar F, Haghpanah T, Babaee A, Eftekhar-Vaghefi SH. The Effects of Olive Leaf Extract on The Testis, Sperm Quality and Testicular Germ Cell Apoptosis in Male Rats Exposed to Busulfan. Int J Fertil Steril 2019;13(1):57-65. DOI:10.22074/ijfs.2019.5520.

45. Sahin Z, Ozkaya A, Cuce G, Uckun M, Yologlu E. Investigation of the effect of naringenin on oxidative stress-related alterations in testis of hydrogen peroxide-administered rats. J Biochem Mol Toxicol 2017;31(9):21928. DOI:10.1002/jbt.21928.

46. Richburg JH, Murphy C, Myers JL. The Sertoli cell as a target for toxicants. DOI: 10.1016/B978-0-12-801238-3.02137-1

47. Chen X, Liang M, Wang D. Progress on the study of the mechanism of busulfan cytotoxicity. Cytotechnology. 2018 Apr;70:497-502.DOI:

48. Cai Y, Liu T, Fang F, Shen S, Xiong C. Involvement of ICAM-1 in impaired spermatogenesis after busulfan treatment in mice. Andrologia 2016;48(1):37-44. DOI:10.1111/and.12414.

49. Jiang S, Xu Y, Fan Y, Hu Y, Zhang Q, Su W. Busulfan impairs blood-testis barrier and spermatogenesis by increasing noncollagenous 1 domain peptide via matrix metalloproteinase 9. Andrology 2022;10(2):377-91. DOI:10.1111/andr.13112.

50. Zhao L, Zhao J, Dong Z, Xu S, Wang D. Mechanisms underlying impaired spermatogenic function in orchitis induced by busulfan. Reprod Toxicol 2023;115:1-7. DOI:10.1016/j.reprotox.2022.11.002.

51. Garza S, Papadopoulos V. Testosterone recovery therapy targeting dysfunctional Leydig cells. Andrology 2023;11(5):816-25. DOI:10.1111/andr.13304.

52. Dutta S, Majzoub A, Agarwal A. Oxidative stress and sperm function: A systematic review on evaluation and management. Arab J Urol 2019;17(2):87-97. DOI :10.1080/2090598x.2019.1599624.

53. Moussa EM, Kelada Ip, Safwat SH, Sawires SK. Comparative Study of The Therapeutic Potential of Bone Marrow-derived Mesenchymal Stem Cells Versus Their Secreted Vesicles on Renal Corpuscles of Rats with Diabetic Nephropathy: A Histological, Biochemical and Morphometric Study. Egypt J Histol 2023;46(4):1806-36. DOI:10.21608/ejh.2022.151488.1731.

54. Fischer UM, Harting MT, Jimenez F, Monzon-Posadas WO, Xue H, Savitz SI, *et al*. Pulmonary passage is a major obstacle for intravenous stem cell delivery: the pulmonary first-pass effect. Stem Cells Dev 2009;18(5):683-92. DOI:10.1089/scd.2008.0253.

55. Atalla S, Saleh H, Abdel Gawad S, Mohamed H. Histological study on the effect of adipose tissue-derived mesenchymal stem cells on the testis of chemically induced castration model by calcium chloride in adult albino rats. Egypt J Histol 2017;40(4):486-96. DOI:10.21608/ejh.2017.5689.

56. Payehdar A, Hosseini SE, Mehrabani D. Histomorphometric and Histological Assessments of Transplantation of Adipose Tissue-Derived Stem Cells in Busulfan-Induced Azoospermic Testis of Mice. Adv Hum Biol 2023;13(2):192-8.

57. Li J, Wu Z, Zhao L, Liu Y, Su Y, Gong X, *et al*. The heterogeneity of mesenchymal stem cells: an important issue to be addressed in cell therapy. Stem Cell Res Ther 2023;14(1):381. DOI:10.1186/s13287-023-03587-y.

58. Monsefi M, Fereydouni B, Rohani L, Talaei T. Mesenchymal stem cells repair germinal cells of seminiferous tubules of sterile rats. Iran J Reprod Med 2013;11(7):537-44.

59. Tamadon A, Mehrabani D, Rahmanifar F, Jahromi AR, Panahi M, Zare S, *et al*. Induction of Spermatogenesis by Bone Marrow-derived Mesenchymal Stem Cells in Busulfan-induced Azoospermia in Hamster. Int J Stem Cells 2015;8(2):134-45. DOI:10.15283/ijsc.2015.8.2.134.

60. Van Saen D, Goossens E, De Block G, Tournaye H. Bone marrow stem cells transplanted to the testis of sterile mice do not differentiate into spermatogonial stem cells and have no protective effect on fertility. Fertil Steril 2009;91(4 Suppl):1549-52. DOI:10.1016/j.fertnstert.2008.09.036.

61. Hassen MT, Mohamed HK, Montaser MM, El-Sharnouby ME, Awad N, Ebiya RA. Molecular, Immunomodulatory, and Histopathological Role of Mesenchymal Stem Cells and Beetroot Extract on Cisplatin Induced Testicular Damage in Albino Rats. Animals (Basel) 2021;11(4). DOI:10.3390/ani11041142.

62. Abd El-Salam S, faruk e, Manawy SM, Nafie NY. Microscopic Structural Alterations in Response to Mesenchymal Stem Cells Injection in Experimentally Induced Oligospermia in Adult Rat Testis (Histological and Immunohistochemical Study). Egypt J Histol 2019;42(4):826-37. DOI:10.21608/ejh.2019.7960.1080.

63. Khalil MR, El-Demerdash RS, Elminshawy HH, Mehanna ET, Mesbah NM, Abo-Elmatty DM. Therapeutic effect of bone marrow mesenchymal stem cells in a rat model of carbon tetrachloride induced liver fibrosis. Biomed J 2021;44(5):598-610. DOI:10.1016/j.bj.2020.04.011.

64. Zickri MB, Moustafa MH, Fasseh AE, Kamar SS. Antioxidant and antiapoptotic paracrine effects of mesenchymal stem cells on spermatogenic arrest in oligospermia rat model. Ann Anat 2021;237:151750. DOI:10.1016/j.aanat.2021.151750.

65. Rasouli M, Naeimzadeh Y, Hashemi N, Hosseinzadeh S. Age-Related Alterations in Mesenchymal Stem Cell Function: Understanding Mechanisms and Seeking Opportunities to Bypass the Cellular Aging. Curr Stem Cell Res Ther 2024;19(1):15-32. DOI:10.2174/1574888x18666230113144016.

66. Cai YT, Xiong CL, Liu TS, Shen SL, Rao JP, Qiu F. Secretions released from mesenchymal stem cells improve spermatogenesis restoration of cytotoxic treatment with busulfan in azoospermia mice. Andrologia 2021;53(8):e14144. DOI:10.1111/and.14144.

67. Guo XB, Zhai JW, Xia H, Yang JK, Zhou JH, Guo WB, *et al*. Protective effect of bone marrow mesenchymal stem cell-derived exosomes against the reproductive toxicity of cyclophosphamide is associated with the p38MAPK/ERK and AKT signaling pathways. Asian J Androl 2021;23(4):386-91. DOI:10.4103/aja.aja_98_20.

68. Ma Y, Zhou Y, Zou SS, Sun Y, Chen XF. Exosomes released from Sertoli cells contribute to the survival of Leydig cells through CCL20 in rats. Mol Hum Reprod 2022;28(2):gaac002. DOI:10.1093/molehr/gaac002.

69. Zhou Y, Yan J, Qiao L, Zeng J, Cao F, Sheng X, *et al*. Bone Marrow Mesenchymal Stem Cell-Derived Exosomes Ameliorate Aging-Induced BTB Impairment in Porcine Testes by Activating Autophagy and Inhibiting ROS/NLRP3 Inflammasomes via the AMPK/mTOR Signaling Pathway. Antioxidants 2024;13(2):183. DOI:10.3390/antiox13020183.

70. Meligy FY, Abo Elgheed AT, Alghareeb SM. Therapeutic effect of adipose-derived mesenchymal stem cells on Cisplatin induced testicular damage in adult male albino rat. Ultrastruct Pathol 2019;43(1):28-55. DOI:10.1080/01913123.2019.1572256.

71. Gao H, Cao H, Li Z, Li L, Guo Y, Chen Y, *et al*. Exosome-derived Small RNAs in mouse Sertoli cells inhibit spermatogonial apoptosis. Theriogenology 2023;200:155-67. DOI:10.1016/j.theriogenology.2023.02.011.

72. Liu Y, Holmes C. Tissue Regeneration Capacity of Extracellular Vesicles Isolated From Bone Marrow-Derived and Adipose-Derived Mesenchymal Stromal/Stem Cells. Front Cell Dev Biol 2021;9:648098. DOI:10.3389/fcell.2021.648098.

73. Zhang W, Yang C, Guo W, Guo X, Bian J, Zhou Q, *et al*. Rotective effect of bone marrow mesenchymal stem cells-derived exosomes against testicular ischemia-reperfusion injury in rats. Nan Fang Yi Ke Da Xue Xue Bao 2018;38(8):910-6. DOI:10.3969/j.issn.1673-4254.2018.08.02.

74. Zhang X, Song D, Kang H, Zhou W, Chen H, Zeng X. Seminal plasma exosomes evoke calcium signals via the CatSper channel to regulate human sperm function. BioRxiv 2020;5:1-41. DOI:10.1101/2020.05.21.094433.

75. Thirouard L, Holota H, Monrose M, Garcia M, De Haze A, Saru JP, *et al*. Analysis of the Reversible Impact of the Chemodrug Busulfan on Mouse Testes. Cells 2021;10(9):403. DOI:10.3390/cells10092403.

76. Mitchell R. The cell as a unit of health and disease. In: Kumar V, Abbas AK, Aster JC, (eds). Robbins and Cotran pathologic basis of disease. 10th ed. New York: Elsevier Health Sciences; 2018. 1-30.

77. Thanh TN, Van PD, Cong TD, Le Minh T, Vu QHN. Assessment of testis histopathological changes and spermatogenesis in male mice exposed to chronic scrotal heat stress. J Animal Behav Biometeorol 2020;8(3):174-80. DOI:10.31893/jabb.20023.

78. Xiao J, Wan W, Zhang Y, Ma J. Administration of Dexmedetomidine Does Not Produce Long-Term Protective Effect on Testicular Damage Post Testicular Ischemia-Reperfusion Injury. Drug Des Devel Ther 2021;15:315-21. DOI:10.2147/dddt.s293926.

الملخص العربى

دراسة هستولوجية عن التأثيرالعلاجي المحتمل للخلايا الجذعية الوسطية المشتقة من النخاع العظمى مقابل حويصلاتها المفرزة خارج الخلية علي الأنابيب الناقلة للمني في الجرذان بعد السمية المحدثة بالبوسلفان

ريهام عبدالله محمد عبدالرحمن، نادية امين شرف الدين، مشيرة احمد زهير، اماني عبدالمنعم سليمان

قسم علم الانسجة وبيولوجيا الخلية ، كلية الطب ، جامعة الإسكندرية

المقدمة: عقار البوسلفان هو أحد عناصر العلاج الكيميائي ، والذى] يستخدم بشكل روتينى لإحداث فقر دم حاد لدى مرضى سرطان الدم، يؤدي للأسف إلى العقم لدى الناجين من السرطان. ظهرت الخلايا الجذعية الوسطية المشتقة من النخاع العظمي وحويصلاتها المفرزة خارج الخلية كطرق علاج واعدة لعلاج الخصية بعد السمية المحدثة بواسطة البوسولفان.

الهدف: مقارنة التأثير العلاجى المحتمل للخلايا الجذعية الوسطية المشتقة من النخاع العظمى وحويصلاتها المفرزة خارج الخلية في تخفيف هذه التغييرات الهيستولوجية والكيميائية المحثة بالبوسلفان علي الأنابيب الناقلة للمني.

المواد والطرق: تم استخدام ستة ذكور جرذان بيضاء صغيرة فى عزل الخلايا الجذعية الوسطية المشتقة من النخاع العظمى والحويصلات المفرزة خارج الخلية. تم تقسييم ثمانية وخمسون من ذكور الجرذان البيضاء البالغة على النحو التالى: المجموعة الأولى (المجموعة الظابطة) ٢٤ جرذا مقسمة بالتساوي إلى ٣ مجموعات فرعية IB ،IAوIC، والمجموعة الثانية تلقت بوسلفان ٤٠ مجم / كجم من وزن الجسم عن طريق الحقن داخل الغشاء البريتونى لمرة واحدة والمجموعة الثالثة تلقت الخلايا الجذعية الوسطية المشتقة من النخاع العظميx١ ١٠٦ عن طريق الحقن لمرة واحدة فى القنوات الراجعة لكل خصية والمجموعةالرابعة تلقت الحويصلات المفرزة خارج الخلية ٤٠ ميكروجم/مل عن طريق الحقن لمرة واحدة فى القنوات الراجعة لكل خصية والمجموعة الخامسة مجموعة التعافى التلقائي تم تركهم بدون أى تدخل آخر. تم التضحية بالجرذان بعد ٢٨ يوم، وتم تجميع عينات الدم وانسجة الخصية لتحليلها كيميائيا. كما تم اخذ عينات من السائل المنوى لعد الحيوانات المنوية و نسبة الحيوانات المنوية المتحركة.وايضاً تحضير الخصيات و فحصها بالمجهر الضوئي والإلكتروني و حساب مقياس جونسين. تم اجراء التحليل الاحصائى للبيانات التى تم الحصول عليها.

النتائج: نجم عن عقار البوسلفان احداث فجوات مع فقد في الخلايا المبطنة للأنابيب الناقلة للمنى. وتقريبا فراغ تجويفها. بالإضافة إلى ذلك شوهد اضطراب حاجز الخصية الدموي وتغيرات تنكسية لخلايا سيرتولي. كما لوحظ احصائيا انخفاض كبير في مستوى هرمون التستوستيرون في الدم ودلالات مضادات الاكسدة و مقياس جونسين ومعلمات السائل المنوى بالاضافة الى الارتفاع الملحوظ احصائيا لعوامل الأكسدة. نتج عن العلاج ب الخلايا الجذعية الوسطية المشتقة من النخاع العظمي تحسن التغيرات النسيجية في الأنابيب الناقلة للمنى وتحسن العلامات البيوكيميائية ومعلمات السائل المنوى ومع ذلك، أسفرت الحويصلات المفرزة خارج الخليةعن نتائج أفضل.

الخلاصة: أظهرت الحويصلات المفرزة خارج الخلية الجذعية عن نتائج علاجية أفضل من الخلايا الجذعية الوسطية المشتقة من النخاع العظمي في تخفيف إصابة الخصية الناجمة عن بوسولفان.